ADJUSTING STORM-INFLUENCED WIND OBSERVATIONS FOR BAROTROPIC HURRICANE TRACK PREDICTION

by

Wade Douglas Jensen

B.S., Colorado State University
(1973)

Submitted in partial fulfillment
of the requirements for the
degree of

Master of Science

at the

Massachusetts Institute of Technology

February, 1978

Signature of Author .....
Department of Meteorology, January 17, 1978

Certified by .....
Thesis Supervisor

Accepted by .....
Chairman, Department Committee

ADJUSTING STORM-INFLUENCED WIND OBSERVATIONS FOR BAROTROPIC HURRICANE TRACK PREDICTION

by

Wade Douglas Jensen

Submitted to the Department of Meteorology on January 17, 1978, in partial fulfillment of the requirements for the degree of Master of Science.

ABSTRACT

SANBAR, a filtered barotropic prediction model designed by Sanders and Burpee (1968), relies on an analysis of the wind field averaged through the depth of the troposphere for making hurricane track predictions. The previous and present methods of interpreting storm-influenced rawinsonde observations are discussed; and a new procedure, which modifies the influenced data, is introduced for use when storms are within 300 nm of land. It is expected that this procedure will improve the SANBAR forecasts, since the large-scale flow in the storm-influenced region would no longer be constrained to be uniform. Fifty cases from nine tropical storms (1958-1975) were studied. Observations within 85 nm of the storm center were found to be overly sensitive and had to be neglected. This procedure appears capable of specifying the initial storm-track velocity about as well as present subjective practise. It should prove especially useful when erratic tracks occur close to landfall.

Thesis Supervisor: Frederick Sanders

Title: Professor of Meteorology

ACKNOWLEDGEMENTS

The author is grateful to Patrick Y. Lui, whose case-study of hurricane Delia, September 1973, ultimately led to this work. Thanks go to Neil D. Gordon for programming assistance and for helpful discussions and suggestions during the research. I am especially grateful to Professor Frederick Sanders for proposing the topic; for his advice and guidance throughout the study; and most of all, for increasing my interest in meteorology. Much thanks also to Isabelle Kole for drafting figures, and to Janice Jensen for typing the manuscript.

TABLE OF CONTENTS

LIST OF FIGURES

LIST OF TABLES

INTRODUCTION

A filtered barotropic prediction model designed by Sanders and Burpee (1968), known as SANBAR, has been used operationally at the National Hurricane Center (NHC) since late 1968. The model operates on winds averaged with respect to mass through the troposphere and is used to predict tropical cyclone tracks by following minimum stream function and maximum vorticity centers. The assertion is that the storm is "steered" by the larger-scale current in which it is embedded, as suggested by Riehl and Haggard and Sanborn, 1956, and by Jordon, 1952, among others.

Originally, objective analysis was performed on data after subtracting from wind observations near the storm center an idealized, circularly-symmetric vortex specified by the location of its center, and by its maximum wind, eye diameter, and radius of influence. The storm-purged residual winds could then be regarded as a measure of the classical steering effect. All of the parameters except the radius of influence were reasonably well known initially in real time. The radius of influence, however, was subjectively determined, with results that often seemed unsatisfactory. Even after 300 nm was adopted as the nominal value to be used, the operationally calculated residual winds were too often unrealistic.

Pike (1972) reported that SANBAR's performance at the 12 and 24 hour forecast times was much worse than that of the statistical forecast methods for the 1971 Atlantic hurricane

season, though SANBAR outperformed the others in long-range 48 and 72 hour forecasts. For a 24 case sample from the 1971 storms, SANBAR forecasts had an average left bias of 28° and a slow bias of 21%, according to Pike. Williams (1972) and Gaertner (1973) found the slow speed bias but not the directional bias in their forecasts made at MIT.

So Pike devised an approach, known as modified-SANBAR, that relied heavily on persistence of past motion. He discarded all observations within the influence region of the storm and substituted a best available estimate of the observed storm motion instead. Then, after the automated analysis, a vortex wind is added to complete the field to be used in subsequent forecasts. Using the same 24 case sample, Pike's Mod-SANBAR forecasts showed significant improvement, with the directional bias of SANBAR eliminated, and the speed bias reduced. Gaertner confirmed the improvement and for the 1972 hurricane season, the Mod-SANBAR model was put into use at NHC.

Though implementing past storm movements has improved the general performance of the model, Sanders, Pike and Gaertner (1975) felt that a present limitation on forecast accuracy was an "inability to make consistently good use of information contained in soundings made within the region influenced by the storm." Cases where the storm path is smooth are handled well, but the sudden twists and turns of erratic tracks are not predicted. The 12-hour forecast storm trajectory is invariably an extrapolation of the previous

6-hour displacement. Rather than present the forecasters at NHC with a 12-hour prediction so similar to those of the statistical models, which also rely heavily on persistence of past motion for their short range prediction, it is hoped that SANBAR could predict sudden changes in movement more effectively. Forecasters could then subjectively evaluate the validity of the SANBAR prognosis, if and when it differed significantly from the statistical models, before issuing their advisories.

Wind observations in the storm influenced area must be potentially valuable for the prediction of any sudden changes in the movement of a tropical storm. However difficult it has been in the past, some effective method for separating the storm wind contribution from the observed winds is needed. This study is concerned with optimum ways of making such a separation.

DATA PREPARATION AND OBJECTIVE ANALYSIS

The SANBAR model relies on an analysis of wind observations, averaged through the depth of the troposphere, and makes no direct reference to the pressure-height data, where errors in lower latitudes are often as large as natural variability. Rawinsonde data was obtained from Northern Hemisphere Data Tabulations available at MIT. Layer-mean winds at each reporting station were estimated from the winds at the ten mandatory pressure levels in the layer from 1000 mb to 100 mb by the trapezoidal rule

$$\underset{\sim}{\bar{V}}_0 = \frac{1}{900}\left[\sum_{i=1}^{8} \frac{(p_{i-1} - p_{i+1})}{2} \underset{\sim}{V}_i + \frac{(p_0 - p_1)}{2} \underset{\sim}{V}_0 + \frac{(p_8 - p_9)}{2} \underset{\sim}{V}_9\right]$$

where p_0 = 1000 mb, ..., p_9 = 100 mb, and $\underset{\sim}{V}_i$ = the horizontal wind vector for the level specified.

Missing winds at interior levels were interpolated from surrounding levels; winds missing at the top or bottom were given the value of the closest available level. Observations at 1000 mb were found to be the most commonly missing, usually for inland reporting stations. When a sounding reported fewer than two of the lower four levels (1000, 850, 700 and 500 mb) or fewer than two of the upper six levels (400, 300, 250, 200, 150 and 100 mb), it was rejected. Even when wind observations at every 50 mb were available, only the ten mandatory levels were used, following the studies of King (1966) and Ahn (1967), which indicated that the mandatory levels represented an

acceptable vertical sample from which to work.

The idealized, circularly-symmetric tangential wind speed, V_θ , to be subtracted from observations within the storm area is of the form

$$V_\theta = X_1 \left\{ \sin \left[\pi \left(\frac{r}{300} \right)^{X_2} \right] \right\}^{X_3} .$$

for $0 \leq r \leq 300$ nm and $V_\theta = 0$ for $r > 300$ nm ; where $X_1 \equiv KV_{max}$, $X_2 \equiv \frac{\ln(0.5)}{\ln(r_e/300)}$, r is the radial distance from the center, V_{max} is the maximum observed wind speed near the surface, K is the proportionality factor between this wind and the maximum wind averaged through the depth of the troposphere, and r_e is the radial distance of V_{max} from the center. Speeds are in knots, distances in nm, and 300 nm is considered to be the maximum storm influence distance. In the original version of SANBAR, $K = 0.72$ and $X_3 = 1.5$.

The parameters X_1 , X_2 and X_3 are varied, and a method was devised whereby the rawinsonde observations themselves determined which were the "best" values to use. We allow X_1 to vary from 0 to 100; X_2 from 0.15 to 0.43 (r_e ranges from 3 to 60); and X_3 from 0.2 to 4.0. Variation of X_1 (or V_{max}) affects the magnitude of the curves in Figure 1 a). Different values of X_2 lead to a translation of the peak in 1 b), while changing X_3 results in significantly altered shapes, as shown in 1 c).

The best set of parameters is taken to be that combination of values which yields the smoothest set of residual (large-

Fig. 1 a) -- Effect of varying x_1 ; $V_\theta = x_1 \left\{ \sin[\pi (\frac{r}{300})^{0.23}] \right\}^{1.6}$

$r_e = 15$

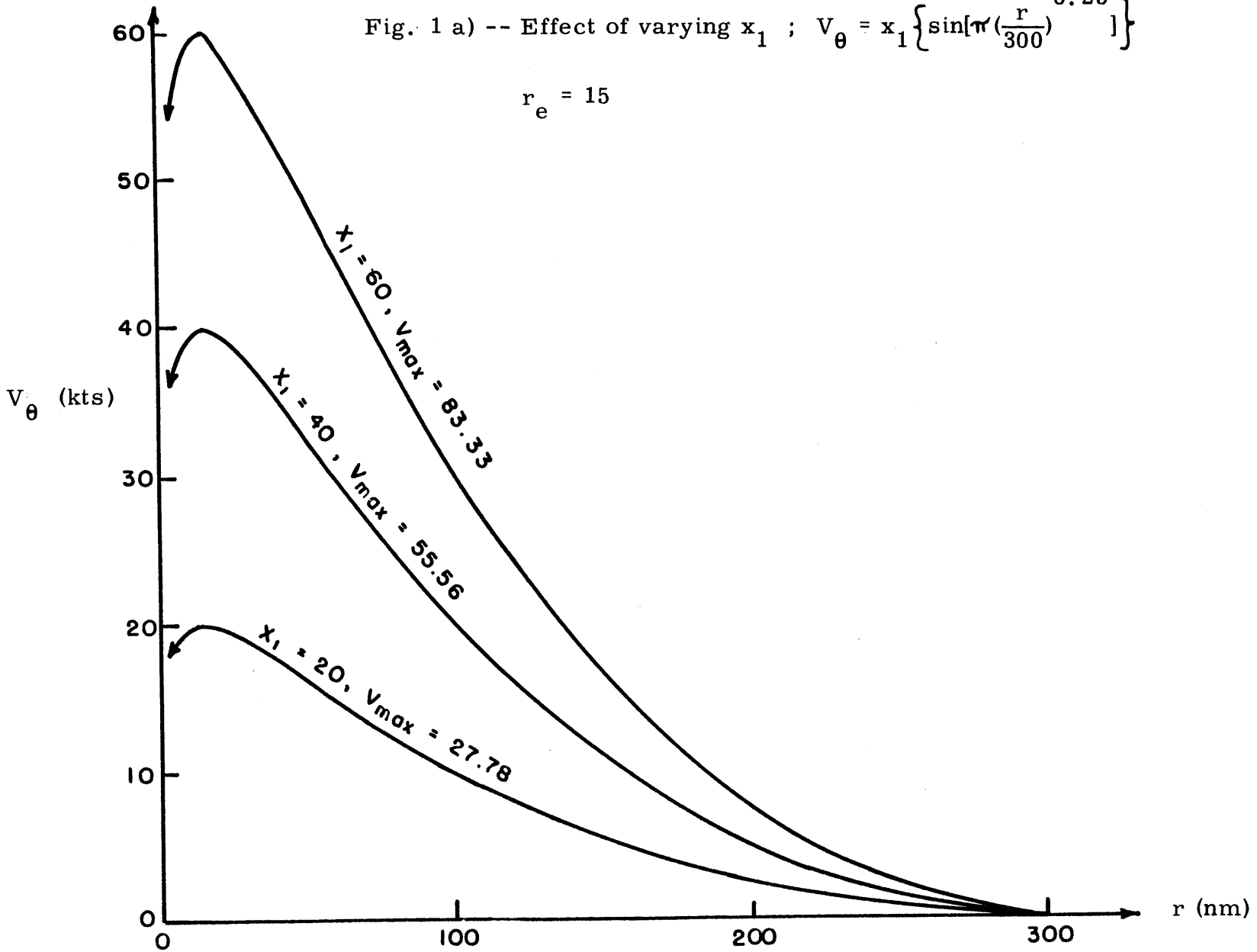

Fig. 1 b) -- Effect of varying x_2 ; $V_\theta = 43.20\left\{\sin[\pi(\frac{r}{300})^{x_2}]\right\}^{1.6}$

$V_{max} = 60$

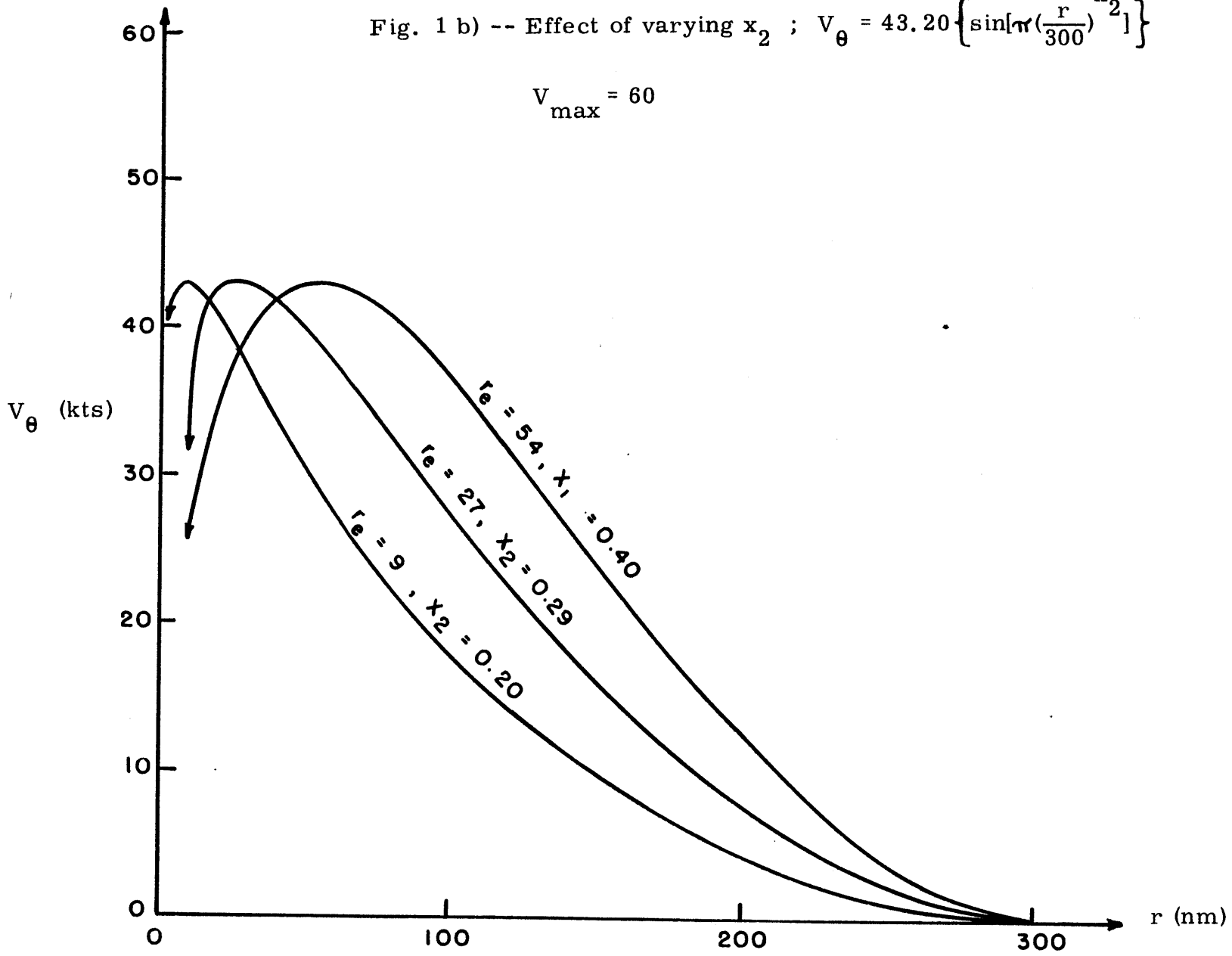

Fig. 1 c) -- Effect of varying x_3 ; $V_\theta = 43.20\left\{\sin[\pi(\frac{r}{300})^{0.23}]\right\}^{x_3}$

$r_e = 15$; $V_{max} = 60$

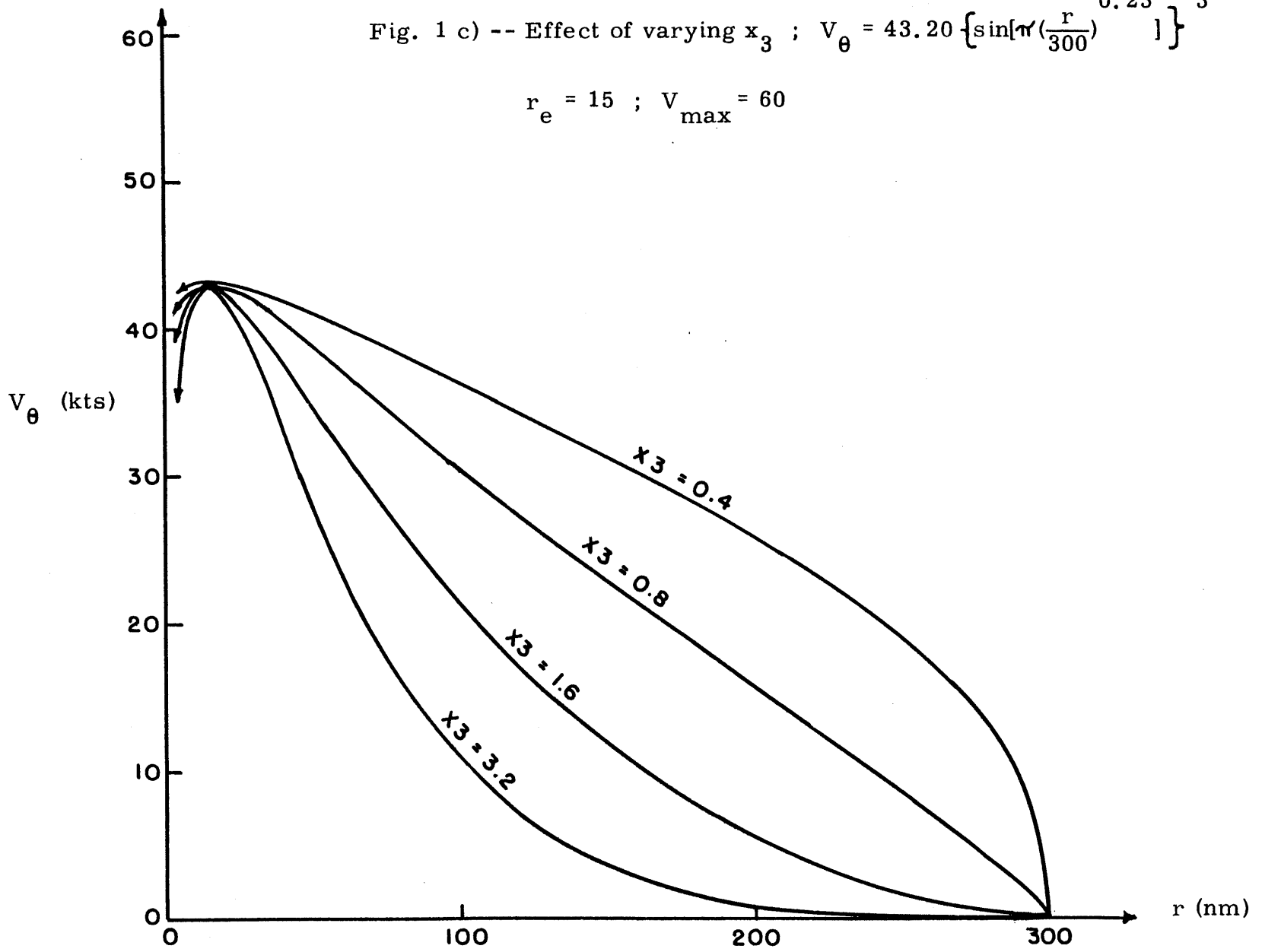

scale) winds defined by $\underset{\sim}{V}_r = \overline{\underset{\sim}{V}}_0 - \underset{\sim}{V}_\theta$, $\overline{\underset{\sim}{V}}_0$ being the layer-mean observed wind. To determine smoothness, an interpolated value of the residual wind is calculated for each station and compared to the actual value of $\underset{\sim}{V}_r$ at that station. This interpolated wind, $\underset{\sim}{V}_p$, is derived from planar fits of the u- and v-components of the residual wind. The planes are determined by the nearest three observing stations which form a triangle enclosing the station in question. Given the latitude, longitude and u- (or v-) component of the residual wind at the vertices, we can compute the interpolated u- (or v-) component of $\underset{\sim}{V}_p$.

Now the deviation, $\underset{\sim}{V}'$, of the actual residual wind from the interpolated residual wind can also be calculated at each station. Notice that observations whose enclosing triangle lies outside the influence region of the storm (300 nm) will always contribute the same value of $\underset{\sim}{V}'$. The best set of parameters for a synoptic case is taken to be that which minimizes the root-mean-square value of $\underset{\sim}{V}'$ over all observing stations except the outermost, which cannot be enclosed by any such triangle. Therefore, the smoothest profile is implicitly the one which minimizes the root-mean-square deviation of those observations which have at least one storm influenced vertice.

In effect, the variability of vortex structure is recognized, and we accomodate the profile to wind observations in the vicinity of the storm. There should be fewer unrealistic residual winds calculated using this method than were calculated

using the original version of SANBAR. Moreover, the method stops far short of specifying the residual winds, as is done in Mod-SANBAR.

Fifty data sets, for nine tropical storms, were chosen for study. They were picked on the basis of at least two simultaneous rawinsonde observations being located within the influence region of the storm. On the average, four such influenced observations were present. Understandably, these storms lay within 300 nm of either the United States coast or parts of the Caribbean islands. As such, they represented especially important forecast problems for NHC. The resulting selection frequencies of the parameters X_1 , X_2 and X_3 are shown in Table 1. Rather surprisingly, in half the instances the implied value of V_{max} is no more than 35 kts*, and the shape of the radial profile is very flat, as evidenced by such small values of X_3 . The current operational SANBAR value of $X_3 = 1.5$ is exceeded only 20% of the time in the present sample! Apparently the tropical storm is often embedded in a weak cyclonic circulation of large scale, and the strongest winds are rarely sampled by the rawinsonde system, leading to these unexpected results. In Table 2 a) it can be seen that the parameters X_1 and X_3 are usually both small or they are both large. Table 2 b) shows that the closer the nearest observing station is to the high energy portion of the storm, the more likely it is that larger values of X_1 and X_3 will

---

* $X_1 \leq 25$ implies $V_{max} \leq 35$ if we assume $K = 0.72$.

Table 1

Frequency of values of parameters chosen to minimize $\underset{\sim}{V}'$

$$V_\theta = X_1\left\{\sin\left[\pi\left(\frac{r}{300}\right)^{x_2}\right]\right\}^{x_3}$$

$$x_1 = 0.72V_{max} \; ; \quad x_2 = \frac{\ln 0.5}{\ln (r_e/300)}$$

x_1(kt)	N	r_e(nm)	N	x_3	N
5	0	3	7	0.2	13
10	8	6	1	0.4	5
15	6	9	5	0.6	3
20	7	12	4	0.8	6
25	4	15	7	1.0	2
30	1	18	1	1.2	6
35	4	21	2	1.4	5
40	2	24	2	1.6	2
45	3	27	2	1.8	2
50	0	30	2	2.0	1
55	0	33	2	2.2	0
60	0	36	1	2.4	0
65	1	39	2	2.6	1
70	2	42	1	2.8	0
75	3	45	1	3.0	2
80	0	48	2	3.2	1
85	2	51	1	3.4	0
90	5	54	1	3.6	0
95	2	57	1	3.8	0
100	0	60	5	4.0	1
Total	50		50		50

Table 2 a)

Interrelationship between x_1 and x_3

x_1 \ x_3	0.2-0.6	0.8-1.8	2.0-4.0	Total
5 - 20	17	4	0	21
25 - 45	4	9	1	14
65 - 95	0	10	5	15
Total	21	23	6	50

Table 2 b)

The effect of the position of the nearest rawinsonde station on the choice of parameters x_1 and x_3

Closest station (nm)	x_3 0.2-0.6	0.8-1.8	2.0-4.0	Total
0 - 50	0	1	1	2
51 - 100	5	6	3	14
101 - 150	3	6	2	11
151 - 200	7	4	0	11
201 - 250	4	3	0	7
251 - 300	2	3	0	5
Total	21	23	6	50

	x_1 5- 20	25- 45	60- 95	Total
0 - 50	0	1	1	2
51 - 100	7	3	4	14
101 - 150	2	5	4	11
151 - 200	7	3	1	11
201 - 250	4	0	3	7
251 - 300	1	2	2	5
Total	21	14	15	50

be chosen. The number of influenced observations did not appear to have any particular relationship to the parameters that were chosen, however.

These dependent features of the parameters X_1 and X_3 are well illustrated by referring to Figure 2, where two quite different storm wind profiles are pictured. Also shown on the profiles are the relative positions of the observing stations for this particular case. The taller curve, with large values of X_1 and X_3, was chosen when the nearby observation at station 72235 was included in the analysis. On the other hand, the flatter curve was picked when that observation was not used. Such flat curves, with the nearest observing station over 150 nm from the storm center, were quite common for our 50 case sample. It seems that the predominance of the smaller values of X_1 and X_3 in Table 1 is therefore at least partly explained by the locations of the nearest rawinsonde stations.

It is also evident that for synoptic cases where storm influenced rawinsonde observations are concentrated at one distance from the storm (as often happens), radically different profiles could have practically identical storm winds at the observation locations. This would be the case when the observing stations happened to cluster near the points of intersection of the profiles. In Figure 2, the maximum discrepancy is only about 5 knots (neglecting station 72235). The locations of the observing stations would certainly seem to be an important factor in determining which values of the parameters are "best". So we should not attach too much importance to the parameter

Fig. 2 -- Two different storm wind profiles are shown, with the observing station positions for hurricane Camille, August 18, 1969, 1200 GMT also given.

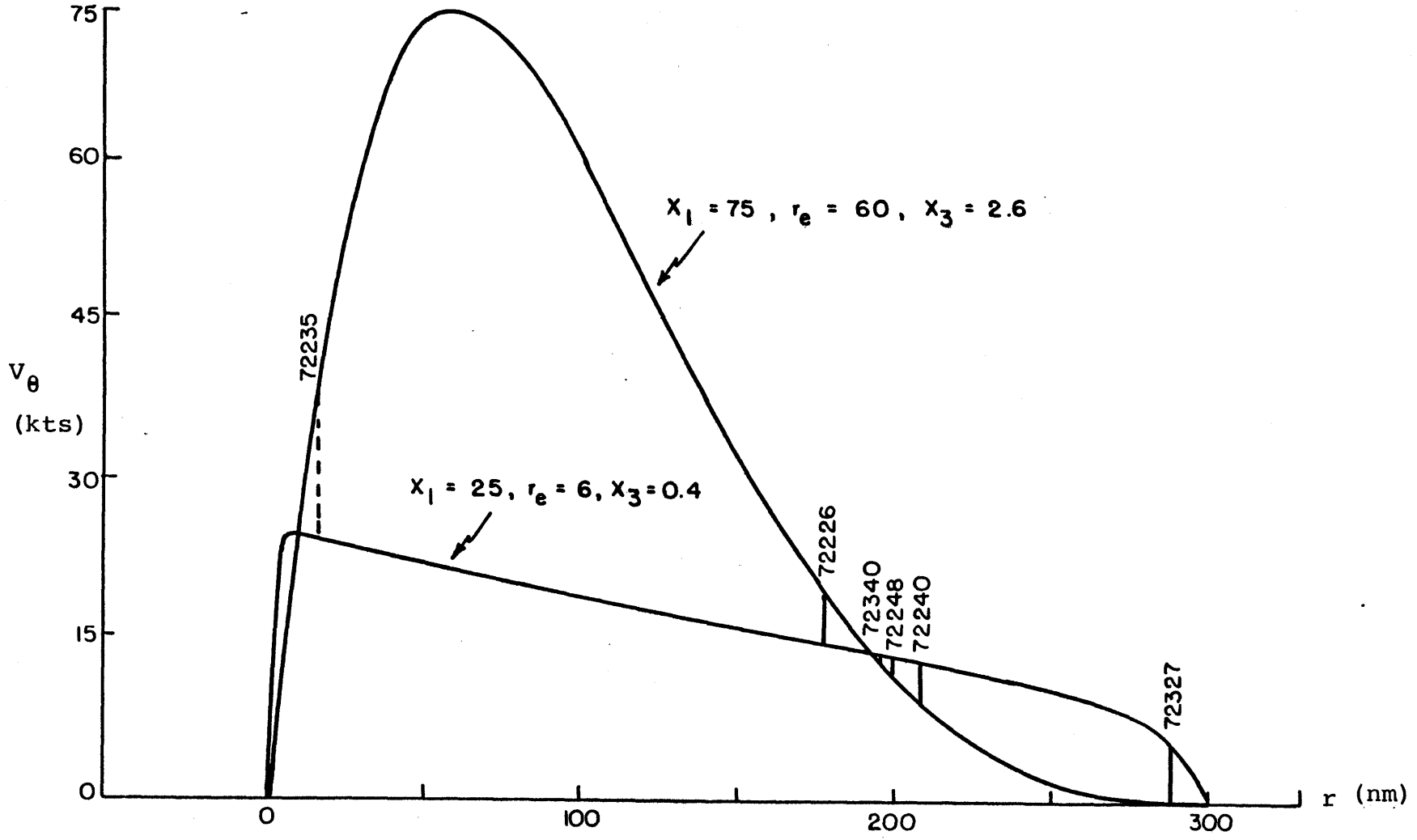

selection frequencies without also taking the observing station locations into account.

Now, the values of the residual wind, $\underset{\sim}{V}_r$, should also provide a good specification of the storm track velocity at the time of the observations. We hope that this specification will be as accurate as the operational estimate made in real time by NHC for the official advisories. So a value of $\underset{\sim}{V}_r$ at the location of the storm center was determined, for the optimum set of storm parameters, by stepwise screening regression for both the zonal and meridional wind components, given the values of $\underset{\sim}{V}_r$ at each observing station.

Any grid-point best estimate of $\underset{\sim}{V}_r$ at the storm grid-point depends on correlations between the hurricane's position and each of the stations, and also upon correlations between stations, since they do not contribute independently to the estimated grid-point value. So correlation coefficients as a function of separation distance were needed. Two samples of soundings used to compute such correlations are shown in Figure 3.

For use in this analysis, an average of those profiles was determined and approximated by the exponential function $r(d) = ae^{-bd^2}$ where $a = 0.93$, $b = 6.0$, and a separation distance of 100 nm means $d = 0.1$. Since this curve only approaches the value of zero asymptotically, it was modified such that $r(d) = 0$ for $d \geq 0.7$ (or 700 nm)*. The present

---

* Note that a similar effect could be produced by including a factor such as $\left[\cos\left(\frac{\pi d}{1.4}\right)\right]^{0.01}$, which has a value near unity for $0 < d < 0.7$, but falls off rapidly to zero at $d = 0.7$.

Figure 3

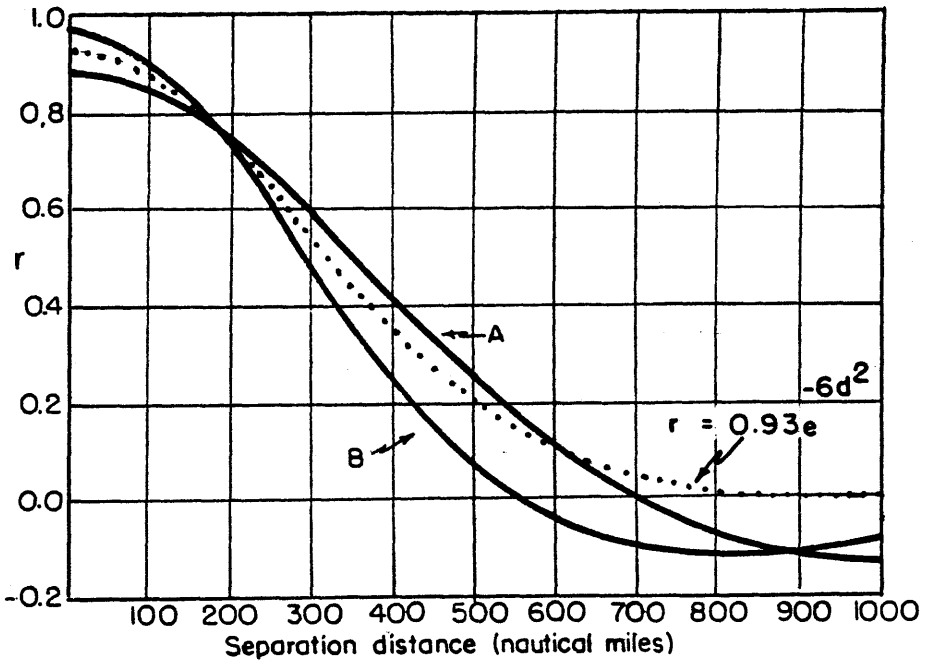

Correlation as a function of separation distance, for departures of vertically-averaged wind from synoptic zonal average value. Curve designated A was derived from a data sample of 1799 soundings on selected hurricane days from 1960 to 1967. Curve designated B was derived from a sample of 1713 soundings from 6-13 September 1971. For the exponential function (dotted curve), d=0.1 corresponds to a separation distance of 100 nm . (All but the exponential function from Sanders et al., 1975.)

analysis makes use of all rawinsonde observations within 700 nm, the distance corresponding to zero correlation.

To compute the regression equations, distances from station to station and from station to hurricane were determined for each case. These distances were then converted to the appropriate correlation coefficients and the symmetric matrix M is constructed (only the upper triangular part is shown),

$$M = \begin{pmatrix} d_1 & r_{1,2} & r_{1,3} & \cdots & r_{1,k} & r_1 \\ & d_2 & r_{2,3} & \cdots & r_{2,k} & r_2 \\ & & d_3 & \cdots & r_{3,k} & r_3 \\ & & & \cdots & \cdots & \cdots \\ & & & & d_k & r_k \\ & & & & & d \end{pmatrix}$$

where r_i is the correlation between the storm and station i, and $r_{i,j}$ is the intercorrelation between stations i and j. Initially $d_1 = d_2 = \ldots = d_k = d = 1.0$.

The matrix is solved by stepwise regression as follows:

1. Choose the station which gives the best specification, as measured by the largest fraction of reduced variance $\frac{r_i^2}{d_i}$. Thus, the first specifier chosen is always the closest station.

2. Eliminate that "specifier" by orthogonalizing the remaining matrix.

$$M^*_{jk} = M_{jk} - \frac{M_{ik}\, M_{ji}}{M_{ii}} \quad \text{for} \quad j \neq i$$

$$M^*_{ik} = \frac{M_{ik}}{M_{ii}}$$

3. Re-examine the new matrix to see which station not already eliminated has the largest fraction of reduced variance and eliminate it in the same manner. Note that these will not necessarily be the best pair of specifiers, because the first is already fixed. This second specifier is the one which, in combination with the first chosen, gives the best specification. Note also that the second specifier need not be the second closest to the hurricane.

4. Re-examine the new matrix for the next specifier. When none of the remaining stations will improve the specification by 1% or more, the elimination process is finished and the regression equation is given in terms of the eliminated variables. The coefficients of the specifiers are the r_i's of the transformed matrix and the fractional unexplained variance is d.

With these specifiers and coefficients, a storm-track velocity can then be computed. For the fifty data sets studied, an average of 4.3 stations were used for this computation, 3.0 with positive coefficients. (Negative coefficients are the result of correlations between stations.) Now, for each

individual synoptic case, a comparison was made between this specified initial track velocity emerging from the regression analysis and an estimate of the actual initial velocity. The estimate was obtained from best track information; namely a tangent to the track with a speed computed by averaging the distances traveled in the preceding and succeeding 12-hour periods. The best tracks were taken from annual Monthly Weather Review articles on the previous hurricane season. Next, a calculation of the errors that would have ensued from using the regression-specified track velocity as a 12-hour extrapolation forecast was made. Then two aspects of the error vectors were examined, using the definitions of Sanders and Gordon (1976), and illustrated in Figure 4.

Early in the work, an unexpected development turned up. Whenever the storm center was rather close to a sounding location, the regression specification was likely to be quite poor. In such instances, slight changes in the storm location led to quite large changes in the direction of $\underset{\sim}{V}_\theta$, and $\underset{\sim}{V}_r$ was therefore quite sensitive to the placement of the hurricane center. Compounding this, these stations also dominated the regression specification due to their closeness. In Table 3, evidence of this relationship between the errors and the distance to the nearest observing station is presented. After some trial and error, 85 nm was decided on as the cutoff between stations we would ignore and those we would use.

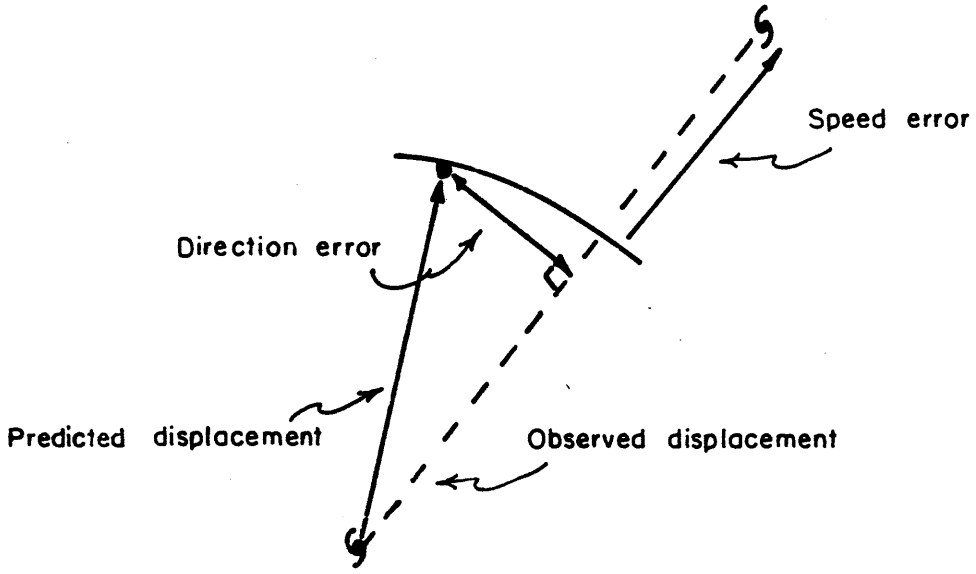

Fig. 4 -- Sketch illustrating speed and direction errors

Table 3

Relationship between errors and the distance to the nearest observing station.

Nearest station (nm)	# of cases	Specification error (kts)	12-hour prediction error (nm)
0- 85	10	7.9	115
86-120	9	4.3	43
121-140	9	4.3	63
141-170	12	3.4	58
171-210	10	4.0	48
211-300	10	5.2	64
Total*	50	4.2	55

* Excluding the cases from 0-85 nm, which were rerun and are are also included in the table

Table 4 illustrates how 85 nm was arrived at as the cutoff. After discarding the nearest rawinsonde observations, and proceeding through the entire process again, the errors were compared. Only the case with an observation at 69 nm exhibited a larger position error, using 85 nm as the cutoff. On the other hand, only one of the six additional cases would have been improved had 100 nm been used as the cutoff.

So the ten cases with observations within 85 nm of the storm center were recalculated, without using these observations, and yielding much improved results. Tables 5 a) and 5 b) are the recalculated versions of Tables 1 and 2, respectively. Figure 5 a) shows one of the rerun cases, in which the error was 9 knots. Moderate changes in the storm position

Table 4

How 85 nm was chosen as the minimum separation distance required before a station will be included in the analysis.

Distance to closest rawinsonde (nm)	Storm	Specification error (kts)		12-hour prediction error (nm)	
		Original	Rerun	Original	Rerun
16	Camille (8-18-69-12Z)	13.4	1.1	165	10
39	Cindy (7-9-59-00Z)	8.8	0.4	140	35
59	Donna (9-11-60-12Z)	7.1	2.8	85	55
60	Delia (9-6-73-12Z)	8.8	3.9	150	70
61	Cindy (7-9-59-12Z)	6.4	7.1	135	100
67	Delia (9-5-73-12Z)	2.1	2.7	85	45
69	Donna (9-12-60-12Z)	3.2	4.6	70	85
71	Ginny (10-25-63-12Z)	14.5	5.0	145	65
78	Gracie (9-23-59-12Z)	5.3	0.0	75	25
81	Eloise (9-23-75-12Z)	9.5	3.5	95	40
87	Gracie (9-24-59-12Z)	3.5	4.2	15	30
89	Gracie (9-23-59-00Z)	2.8	8.8	25	95
Total*		7.9	3.1	115	53

* excluding the cases at 87 and 89 nm

Table 5 a)

Interrelationship between x_1 and x_3 (10 reruns)

x_1	x_3 0.2-0.6	0.8-1.8	2.0-4.0	Total
5 - 20	19	2	0	21
25 - 45	7	8	0	15
65 - 95	0	11	3	14
Total	26	21	3	50

Table 5 b)

The effect of the nearest rawinsonde position on the choice of the parameters x_1 and x_3 (10 reruns)

Closest station (nm)	x_3 0.2-0.6	0.8-1.8	2.0-4.0	Total
0 - 50	0	0	0	0
51 - 100	3	2	1	6
101 - 150	5	8	2	15
151 - 200	12	5	0	17
201 - 250	4	3	0	7
251 - 300	2	3	0	5
Total	26	21	3	50

	x_1 5-20	25-45	60-95	Total
0 - 50	0	0	0	0
51 - 100	3	1	2	6
101 - 150	3	6	6	15
151 - 200	11	5	1	17
201 - 250	3	1	3	7
251 - 300	1	2	2	5
Total	21	15	14	50

of less than 20 nm to the north-northeast can result in a nearly perfect specification! But since the ultimate concern of this study is real time operational forecasting, the rather sensitive Charleston observation was eliminated. In Figure 5 b) the specification error is now less than 1 knot.

Figures 6 and 7 show situations where there are observations at 16 nm and 81 nm from the storm center, respectively. Once again, the improvement shown when these observations were eliminated was substantial. For Figure 6 the specification error was 13 knots, while the rerun error was only 1 knot. Similarly, the specification error for Figure 7 was 5 knots and the rerun specification turned out to be nearly perfect.

So it seems that we are still unable to make constructive use of observations very close to the storm center. Of course, such rawinsonde observations can only be made at substantial hazard to the individuals involved, and are seldom available. But suppose that aircraft dropsondes were made available for use in operational hurricane forecasting. On the basis of our results, placement of the dropsondes from 100 to 180 nm of the storm center would be much more informative for track prediction than releasing them within 50 nm of the center.

The error results, averaged for nine tropical storms, are summarized in Table 6. The mean magnitude of the vector difference was 4.2 knots, a considerable error since the mean estimated velocity was about 10 knots. The average position error was 55 nm, the same as the 12-hour errors shown in Table 7*,

---

* From Director's memo on R and D activities at NHC; July 15, 1977.

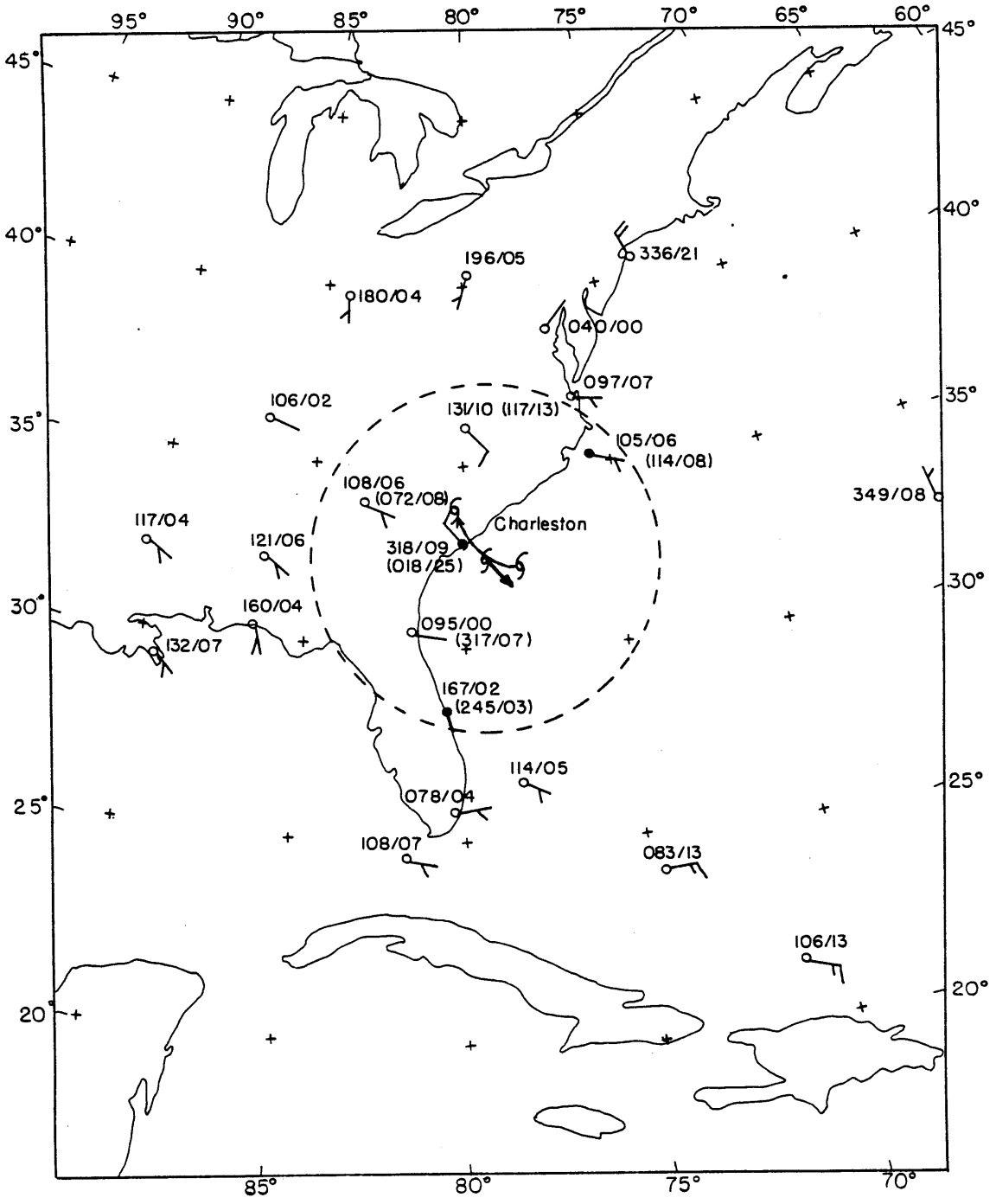

Fig. 5 a) -- Initial mean layer winds for hurricane Cindy, July 9, 1959, 0000 GMT. Hurricane symbols show the position of the storm at successive twelve hour intervals. The heavy arrow represents a twelve hour displacement at the specified velocity. Plotted winds represent $\underset{\sim}{V}_r$, also given by numerical notation. For stations within the influence region of the hurricane (dashed circle), values in parenthesis denote the observed wind, $\underset{\sim}{V}_o$. All winds are indicated in degrees and knots by ddd/ff. Stations with filled circles were used in the regression estimate of the specified velocity.

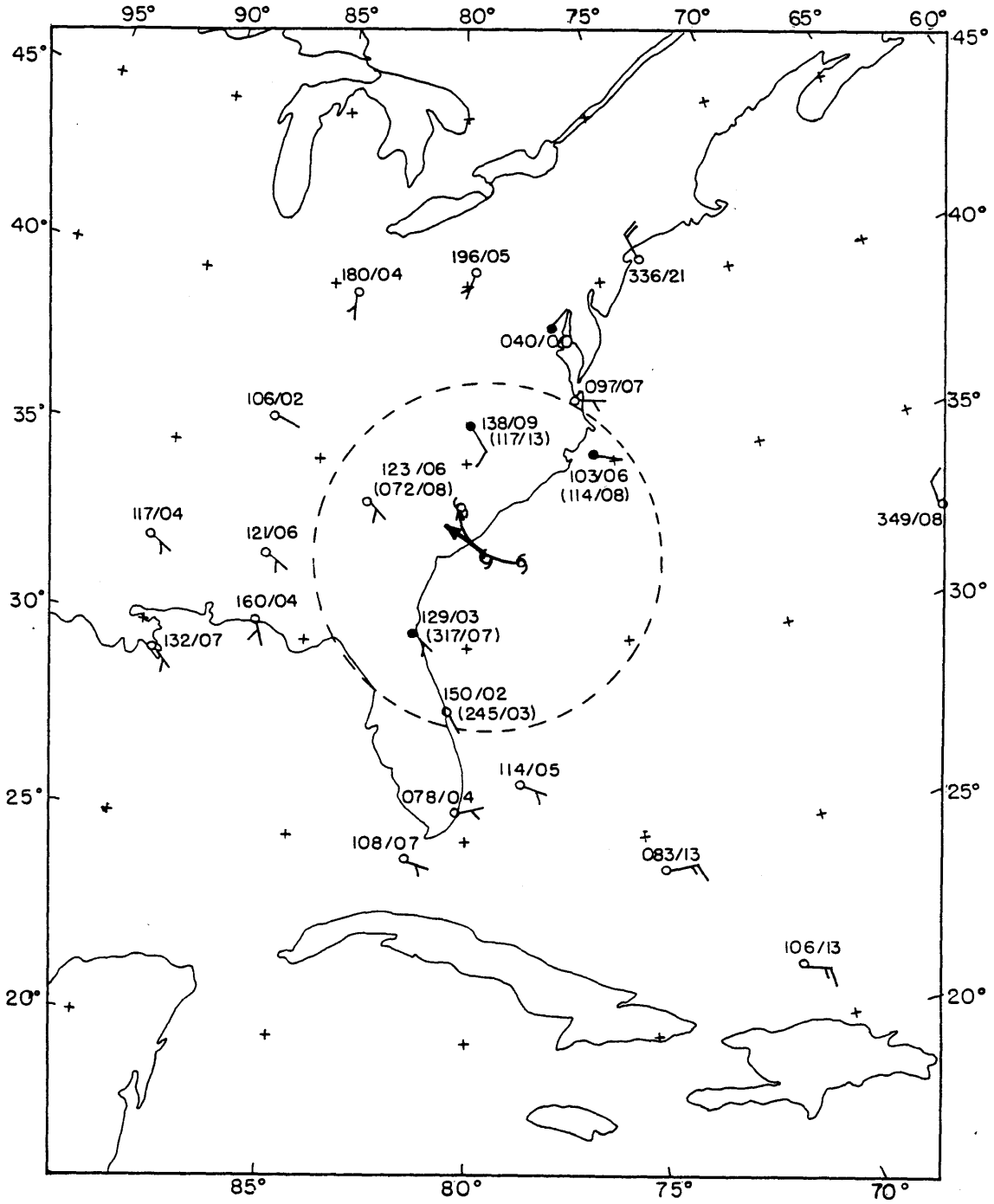

Fig. 5 b) -- Initial mean layer winds for hurricane Cindy, July 9, 1959, 0000 GMT. This analysis excludes the Charleston rawinsonde, located about 40nm from the storm center. Notation same as in Fig. 5 a).

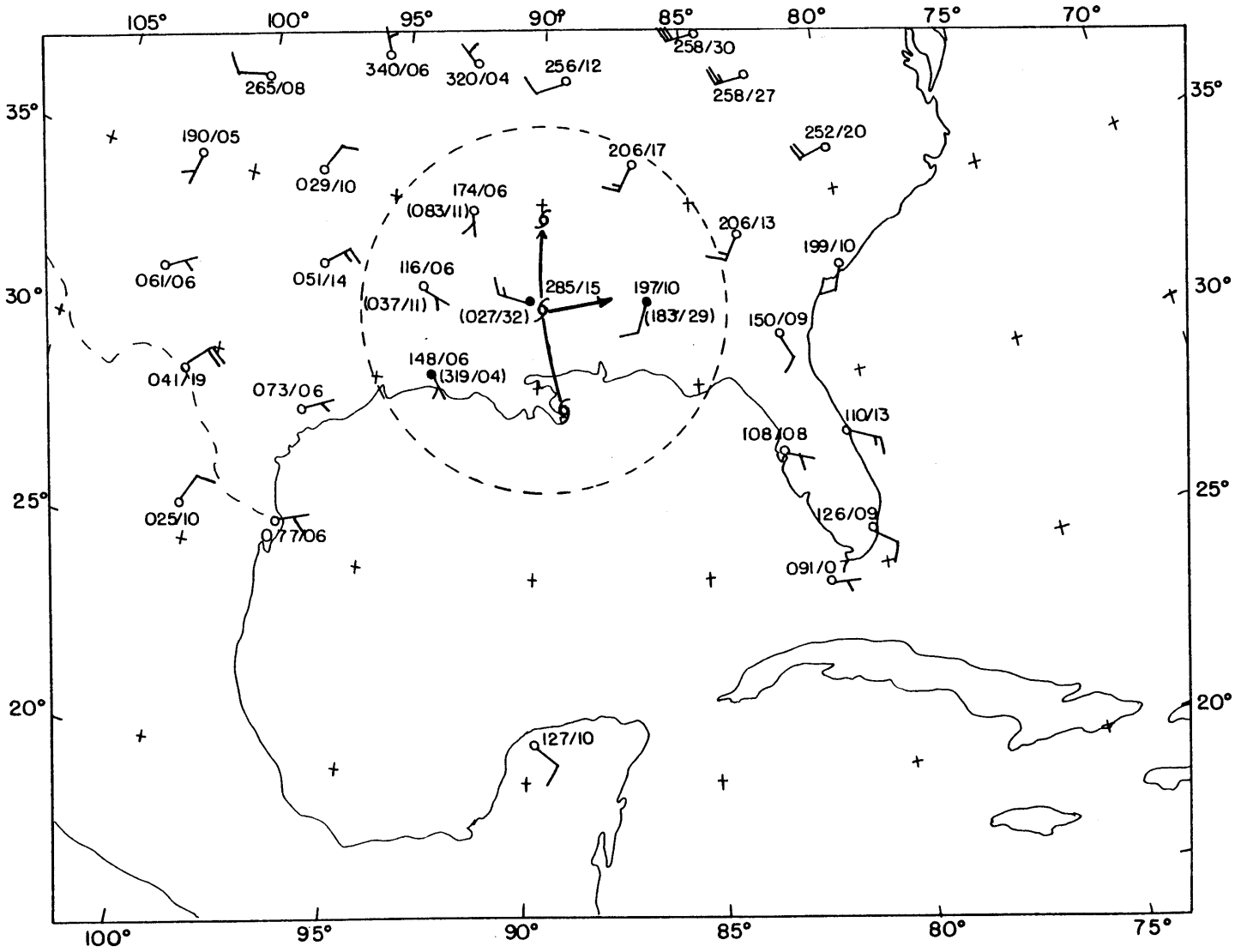

Fig. 6 -- Initial mean layer winds for hurricane Camille , August 18, 1969, 1200 GMT. Notation same as in Fig. 5 a).

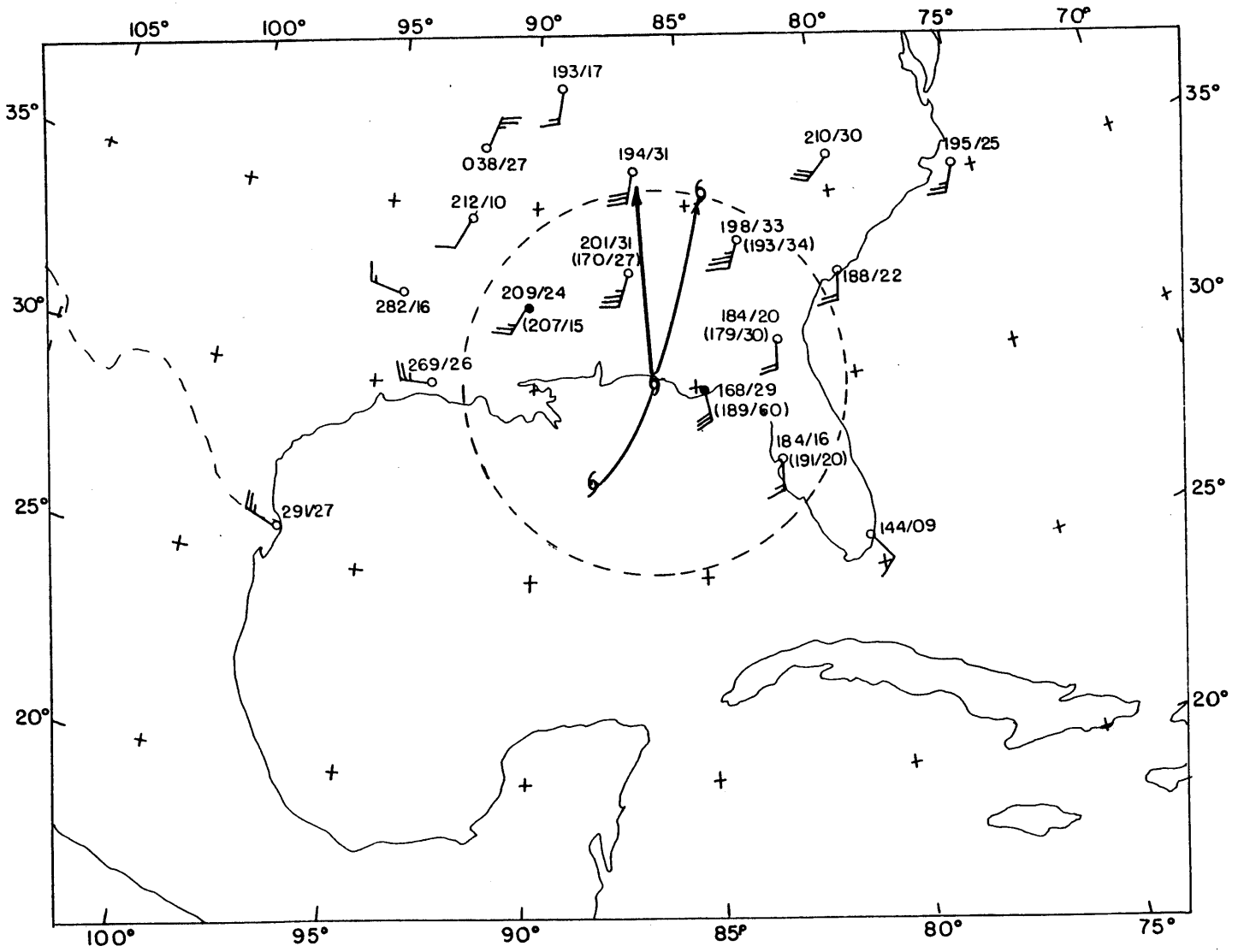

Fig. 7 -- Initial mean layer winds for hurricane Eloise , September 23, 1975, 1200 GMT. Notation same as in Fig. 5 a).

Table 6

Algebraic mean 12-hour forecast and velocity specification errors

Year	Storm	Cases	12-hour forecast errors (nautical miles)*			Track velocity specification errors (knots)*		
			Position	Speed	Direction	Error	Speed	Direction
1958	Helene	6	65.2	1.4	-29.1	5.3	0.8	-1.6
1959	Cindy	4	57.5	-5.3	-36.4	3.6	1.3	-1.9
1959	Gracie	13	43.0	-15.0	7.1	4.0	-1.8	0.8
1960	Donna	10	74.3	-12.2	-17.4	5.0	0.0	-1.4
1963	Ginny	4	62.5	5.4	23.9	4.9	0.5	0.2
1969	Camille	5	36.5	-27.8	-3.6	2.7	-2.1	0.2
1973	Delia	5	57.7	-12.6	30.6	3.0	-1.2	-0.4
1974	Carmen	1	54.8	-46.6	-15.0	5.4	-4.2	-1.7
1975	Eloise	2	32.2	-29.7	-9.1	4.4	1.6	-4.3
	Totals	50	55.3	-12.3	-4.1	4.2	-0.6	-0.6

* Negative values mean too slow a forecast speed, or a forecast position to the left of the observed track.

Table 7

Homogeneous sample of forecast position errors (nm) over the period 1973-1976.

Model	Mean 12-hour error
NHC 67	55
NHC 72	53
CLIPER	55
NHC 73	53
SANBAR	56
Number of cases	206

Table 8

Frequency of errors

Error range: Track velocity (kts)	Frequency	Error range: Position error (nm)	Frequency
0-1.7	7	0 - 20	5
1.8-3.3	9	21 - 40	11
3.4-5.0	14	41 - 60	16
5.1-6.7	11	61 - 80	8
6.8-8.3	4	81 -100	3
8.4-10	3	101 -120	3
10	2	120	4
Total	50	Total	50

but perhaps better than current capability in seasons with more erratic tracks than 1973 to 1976.

In Table 8, the frequency distribution shows that mean operational accuracy was probably exceeded about half the time. The regression procedure, however, occasionally yielded rather large errors. It should be kept in mind that small errors might be the result of things other than good track velocity specification. For instance, slower moving storms could exhibit smaller errors than faster storms merely because of the distances involved, even though the speed and direction might be poorly specified for the former, and rather well specified for the latter.

Next, some plausible sources of error were examined. In Table 9, the number of observations within the influence region of the storm is shown to affect the specification accuracy.

Table 9

Relationship between errors and the number of observing stations within 300 nm of the storm

# of observations	# of cases	Specification error (kts)	12-hour prediction error (nm)
2	10	4.6	49
3	14	4.5	71
4	10	4.3	55
5	9	3.3	51
6	6	4.5	40
7	1	2.1	31
Total	50	4.2	55

This is corroborated by the 12-hour forecast position errors in the same table, allowing that the seemingly better results when only two observations were available is probably a peculiarity of this sample. It should also be kept in mind that the sample cases are not statistically independent, since successive 12-hour situations were studied for 8 of the 9 storms.

It also seemed that an important error source might be the non-uniformity of the observing stations around the storm center. Consider the situation in Figures 8 a) and 8 b), where only the oppositely located stations A and B will be used to compute the specified storm-track velocity. Given the observed winds at A and B, there is only one possible estimated initial velocity! It makes no difference which storm profile is chosen; or whether too much, too little, or just enough storm wind is actually subtracted out. No matter how the observed winds are modified, the hurricane winds will always have cancelling effects, and the estimated hurricane velocity will be implicitly based on the steering flow. The correctness of the estimated velocity would then depend on the correctness of the premise that the storm-wind profile is circularly symmetric, how well the screening regression is able to estimate the large scale flow at the storm center, and how well the storm in fact follows the "steering" principle.

In reality, of course, stations are not uniformly located about a moving storm center. Such storm-influenced stations will generally be located only in that quadrant of the storm

Fig. 8a)

Oppositely located stations A and B used to estimate the storm track velocity.

$\underset{\sim}{V}_0$ = observed wind

$\underset{\sim}{V}_\theta$ = storm wind

$\underset{\sim}{V}_r$ = residual wind = $\underset{\sim}{V}_0 - \underset{\sim}{V}_\theta$

$$\underset{\sim}{V}_r^{\text{storm}} = \frac{1}{2}\underset{\sim}{V}_r^A + \frac{1}{2}\underset{\sim}{V}_r^B$$

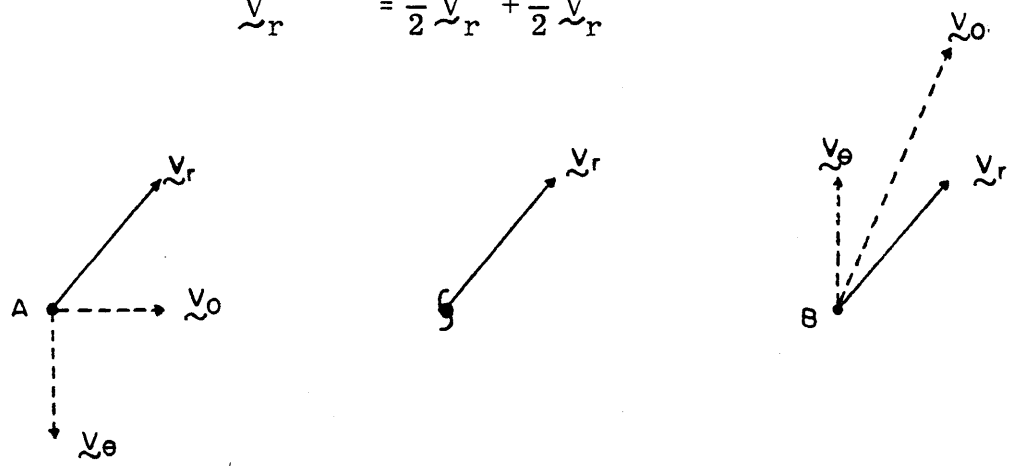

Fig. 8b)

Same observed winds as in a), but $\underset{\sim}{V}_\theta$ is now larger than before.

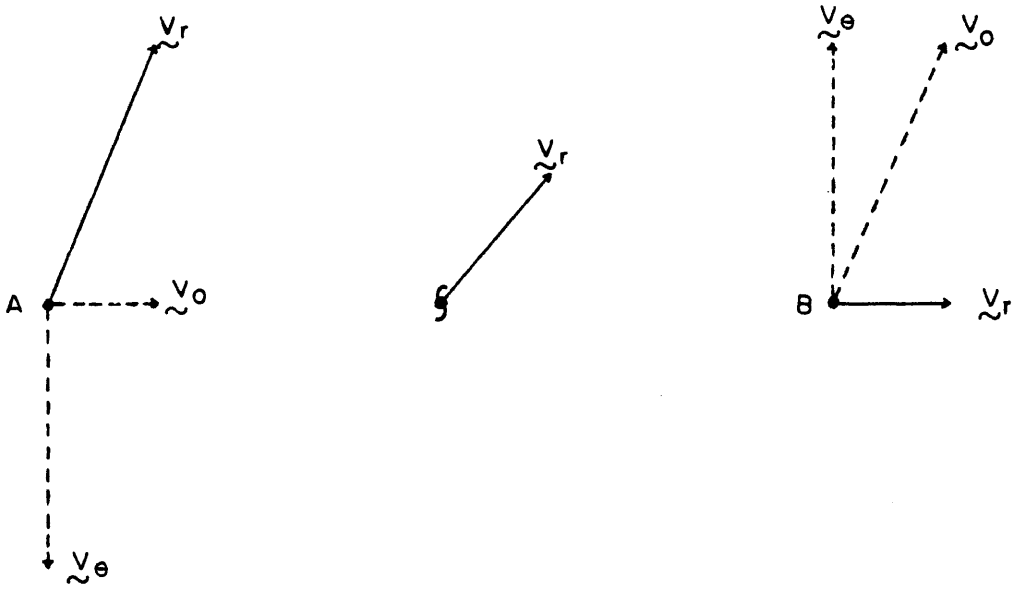

which intersects land. For the 50 case sample, the average angle covered by rawinsondes within 300 nm of the storm center was 137°. In the more realistic situation of Figure 9 a) the stations are no longer oppositely located (though they are still equidistant from the storm center, as a matter of convenience for this argument). As mentioned before, tropical storms often seem to be embedded in a larger scale cyclonic circulation. The regression-computed velocity specification will now depend on how much of that circulation is eliminated from the observations.

First suppose that the large scale steering winds are known to be uniform. In Figure 9 a) these winds are denoted by $\underset{\sim}{V}_e$. If not enough circulation is subtracted out, the residual winds, $\underset{\sim}{V}_r$, certainly differ from the steering winds. But how does this affect $\underset{\sim}{V}_r^{storm}$, the regression-computed velocity specification? Upon examination of the vector difference between $\underset{\sim}{V}_r^{storm}$ and $\underset{\sim}{V}_e$, we notice an interesting characteristic. The direction of the vector discrepancy $\underset{\sim}{V}_r^{storm} - \underset{\sim}{V}_e$ lies within the "range"* of the storm wind directions at the influenced stations, as shown by Figure 9 b). By analogous reasoning, $-(\underset{\sim}{V}_r - \underset{\sim}{V}_e)$, or $\underset{\sim}{V}_e - \underset{\sim}{V}_r$, must lie within that range of storm wind directions when too much storm circulation is subtracted out.

Now the above argument will not be strictly true when observations are not equidistant from the storm. Then there

---

* Range refers to the smallest sector of the circle of storm influence which contains all of the influenced observations.

Fig. 9 a)

Stations A and B located equidistant from the storm center. $\underset{\sim}{V}_e$ is the actual large scale flow, assumed to be uniform.

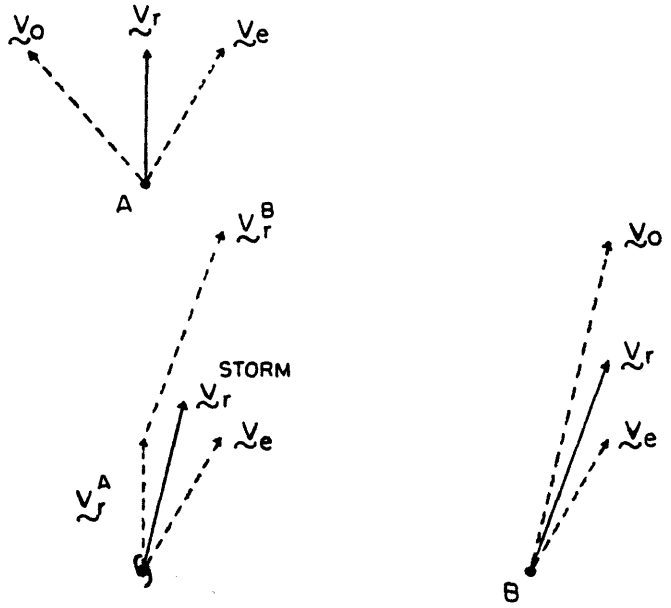

Fig. 9 b)

Comparison of the vector difference between $\underset{\sim}{V}_r^{storm}$ and $\underset{\sim}{V}_e$ with the storm wind direction at stations A and B.

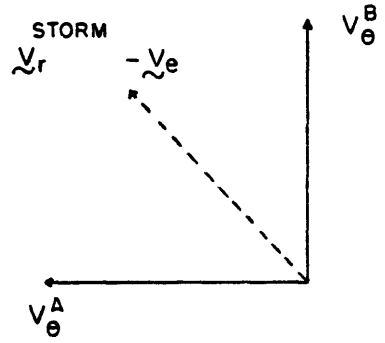

are the additional possibilities that the method could be subtracting too little from the nearer stations and too much from the others (i.e., subtracting a very flat profile); or too much from the nearer stations and not enough from the others (i.e., subtracting a peaked, but rapidly diminishing profile). But these circumstances also seem less likely than the simpler ones of subtracting too much or too little.

So the 25 cases with the largest specification errors were re-examined. In 16 instances, the vector discrepancy, $\underset{\sim}{v}_r^{storm} - \underset{\sim}{v}_e$, was within the range mentioned, implying that not enough hurricane wind had been subtracted away. In fact, for these 16 cases there is some profile which would have given a perfect velocity specification!

But finding those profiles would not improve the objective method of interpreting and modifying storm-influenced winds. Instead, we would like to explain this preference for weaker profiles. Certain reasons immediately come to mind. First, those observations slightly more than 300 nm from the storm become crucially important in the analysis. Since they cannot be modified, any nearby soundings which can be changed will be strongly influenced to take similar values. In Figure 10, this is well illustrated by two clusters of similar residual winds. To the north and west of the storm center, the uninfluenced observations at Cape Hatteras (100/13) and Tampa (056/09) give rise to winds of 064/11 at Jacksonville and 081/10 at Charleston. A similar cluster is seen to the south of the storm center. For this synoptic case, 300 nm does not

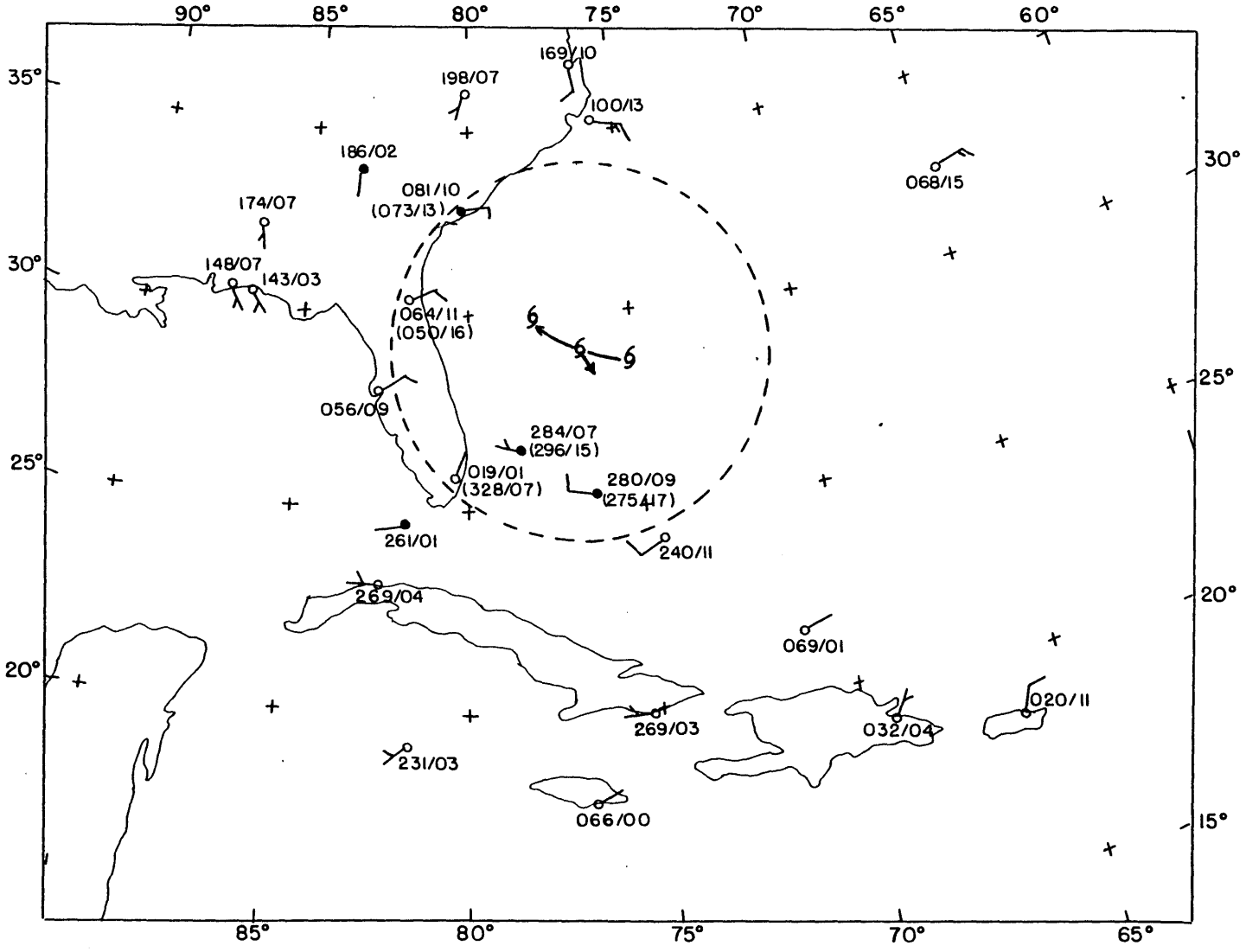

Fig. 10 -- Initial mean layer winds for hurricane Gracie, September 28, 1959, 1200 GMT. Notation same as in Fig. 5 a).

appear to have been a very good choice for the maximum influence distance. Cyclonic circulation is still quite noticeable at both Cape Hatteras and San Salvador (240/11).

Another explanation concerned the extent of rawinsonde stations about the storm. Specification errors were compared to the largest angle not containing any storm influenced observations. We expected the larger errors to occur when there were broad areas with no rawinsondes. Surprisingly, in Table 10 there is not much evidence that a broader angle of coverage resulted in a better specification.

A similar comparison between the errors and the largest angle not containing any stations used in the screening regression specification was made. This was done because these stations would not necessarily be storm influenced, and they should therefore be a good measure of coverage around the storm, not just within 300 nm. Once again though, there was little evidence that broader coverage meant better specification.

Table 10

Velocity specification errors compared to the largest angle not containing any rawinsonde observations within 300 nm of the storm center.

Error (kts)	less than 135°	135°- 179°	180°- 224°	225°- 269°	270° or more	Total
0 - 1.7	0	2	2	3	0	7
1.8 - 3.3	0	3	3	2	1	9
3.4 - 5.0	0	2	5	5	2	14
5.1 - 6.7	1	1	5	2	2	11
6.8 - 8.3	0	1	1	0	2	4
8.4 - 10	0	1	1	1	0	3
> 10	0	0	0	0	2	2
Total	1	10	17	13	9	50

TEST CASES

The individual synoptic cases included in this section are intended to highlight the results of the objective procedure just outlined. Since the previous section dealt with many of the difficulties encountered, some of the better test cases will be presented and discussed here. In Figure 11 there are six storm influenced stations. All six winds are modified rather effectively, and a good specification results from the analysis. Now if Tampa (066/07) or Jacksonville (071/07) had been chosen as predicting stations, the specification would not have been so good. But for the 50 case sample, such a fortuitous choice of predictors is balanced by choices that were not so fortunate.

In Figure 12, the layer-mean winds within 300 nm of the storm center are all modified to south-southeasterly. Both the speed and direction of the storm center are well specified, despite a dearth of observations south of the storm. Generally, the farther north a tropical storm progressed, the better the specifications became, in the Gulf and in the Atlantic. Figures 13 and 14 again show the effectiveness of the modification scheme. A strong southwesterly flow is exhibited by the uninfluenced stations along the middle Atlantic coast. This strong flow is transferred to the influenced stations, and specifications in this region were nearly always quite good. Although the magnitudes of the errors for these cases were sometimes larger than average, the percentage errors were always very small.

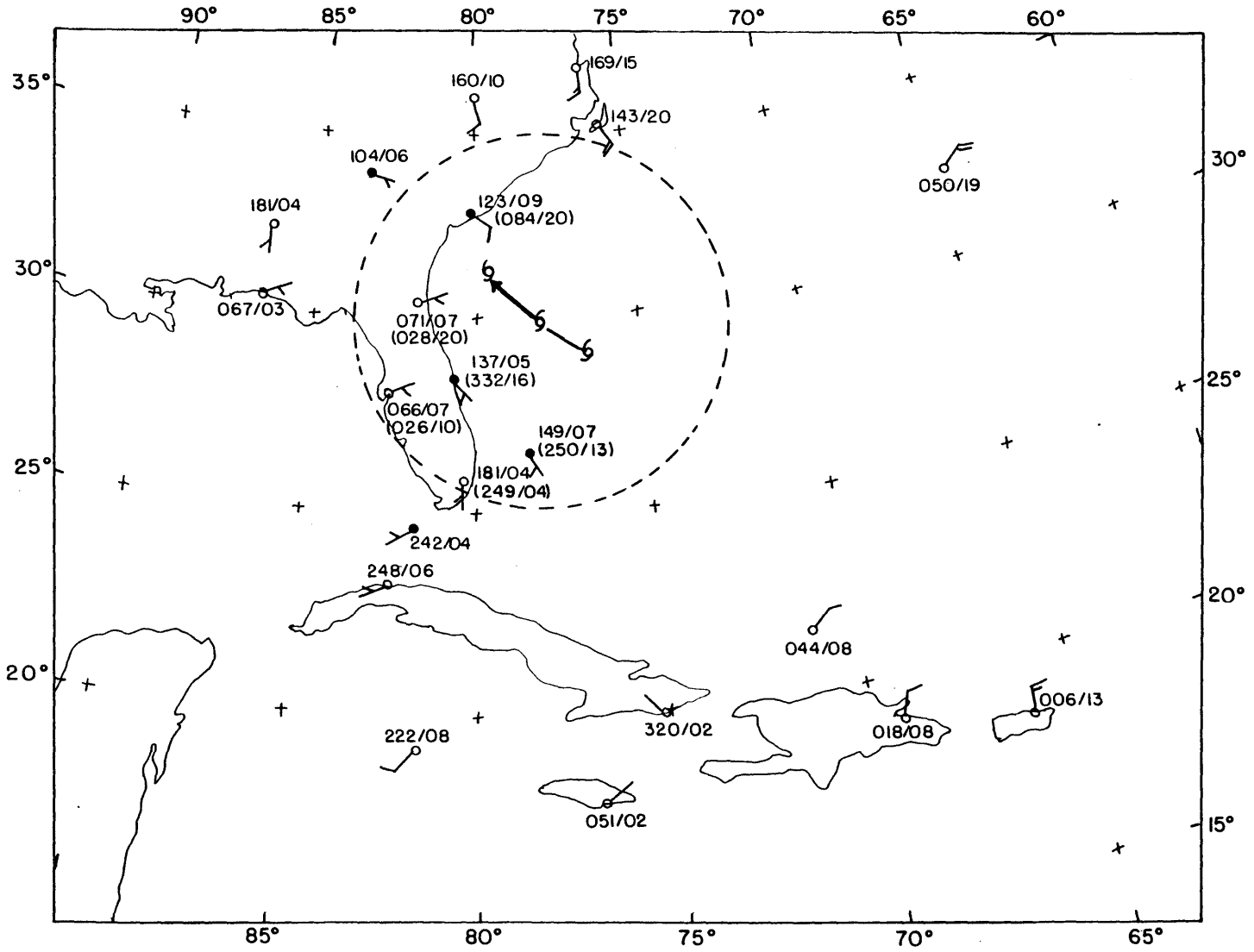

Fig. 11 -- Initial mean layer winds for hurricane Gracie, September 29, 1959, 0000 GMT. Notation same as in Fig. 5 a).

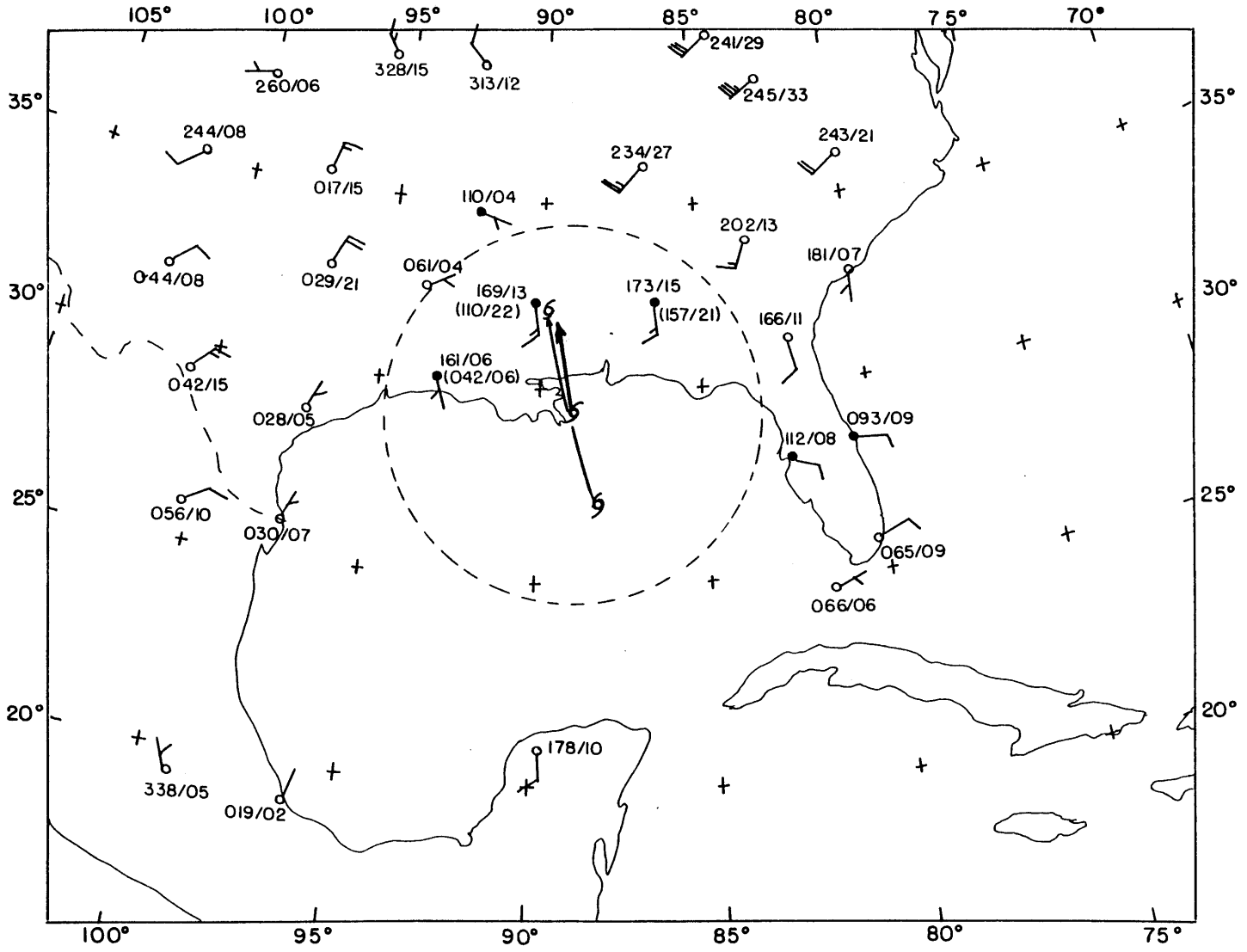

Fig. 12 -- Initial mean layer winds for hurricane Camille, August 18, 1969, 0000 GMT. Notation same as in Fig. 5 a).

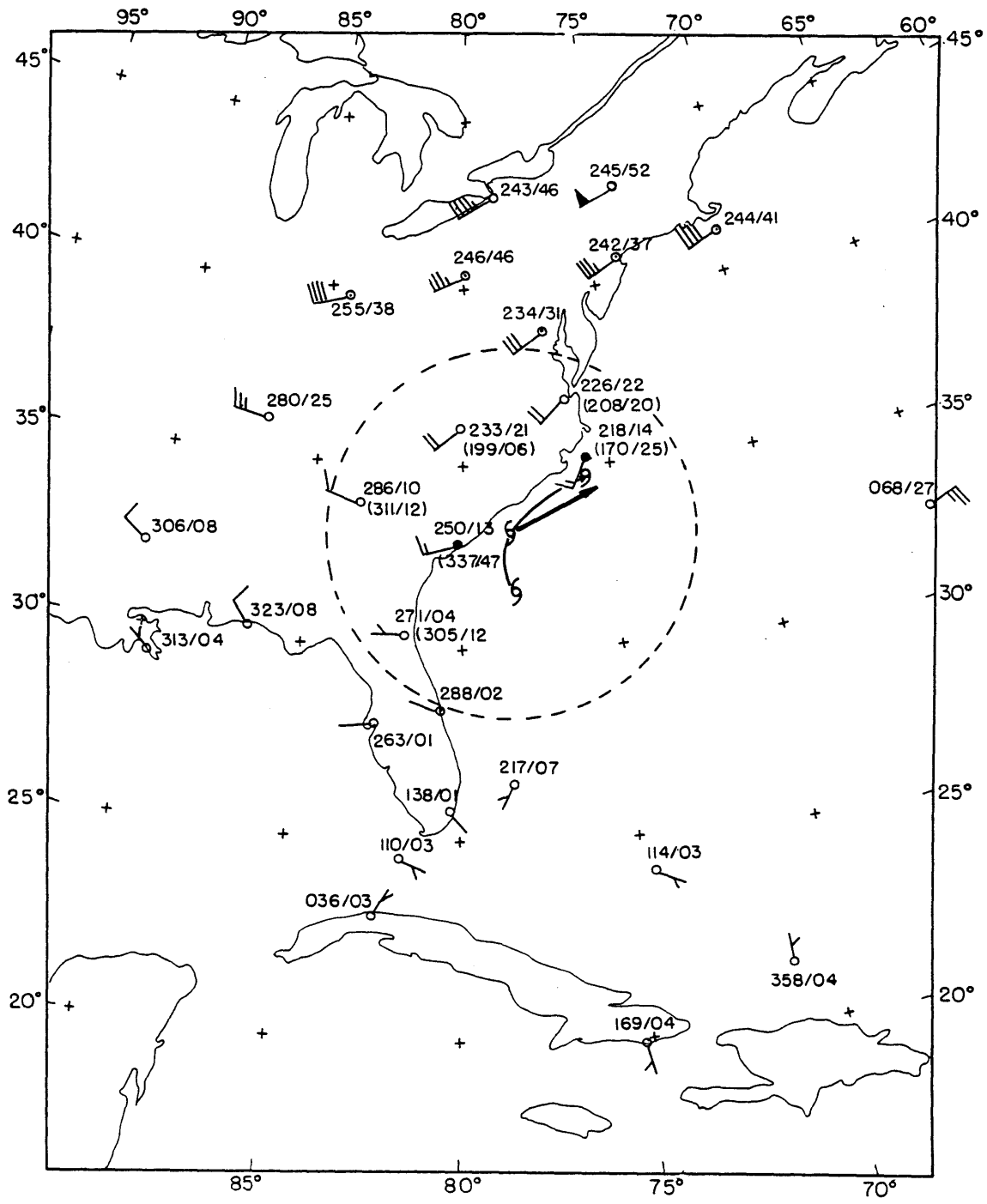

Fig. 13 -- Initial mean layer winds for hurricane Helene, September 27, 1958, 1200 GMT. Notation same as in Fig. 5 a).

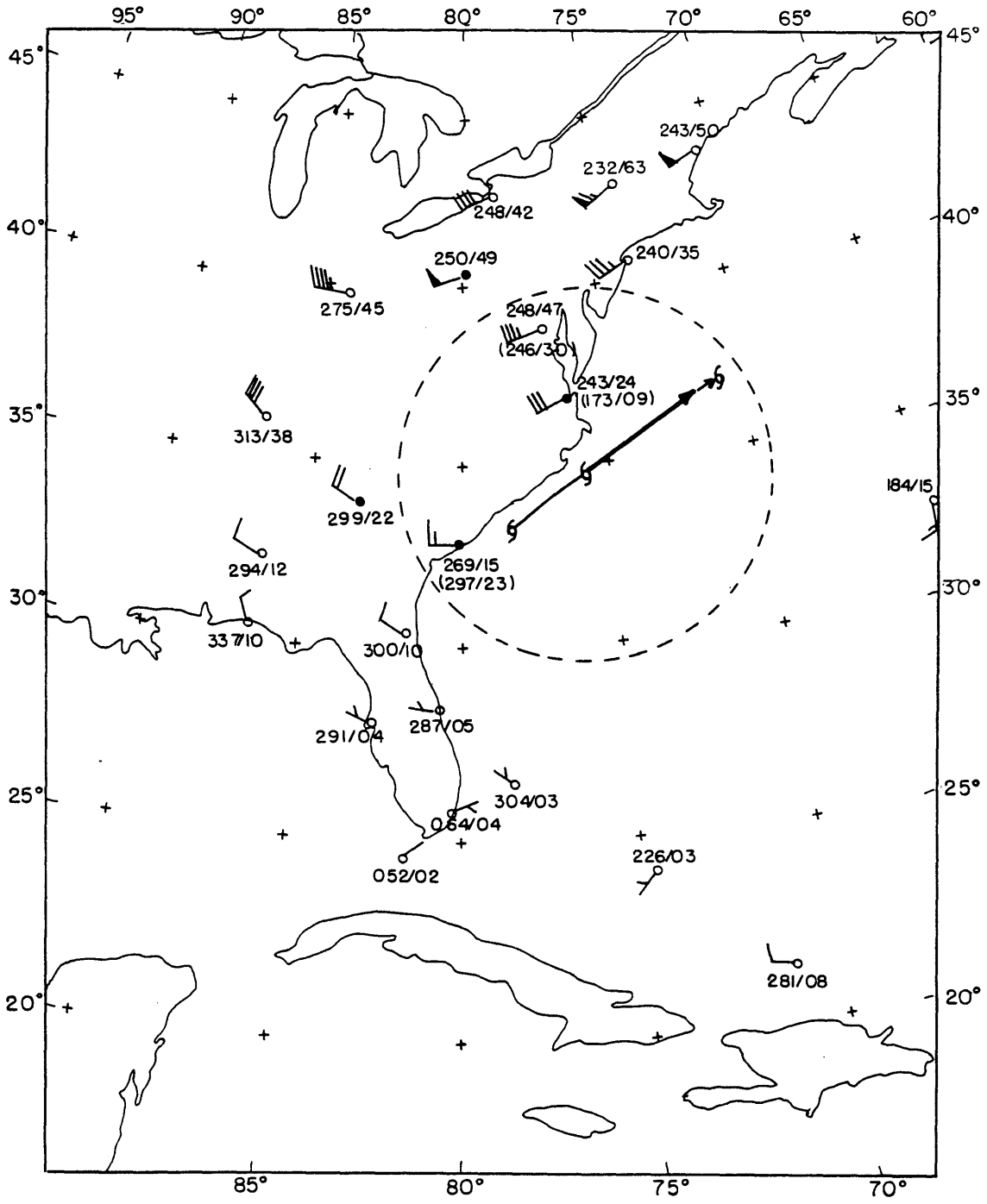

Fig. 14 -- Initial mean layer winds for hurricane Helene, September 28, 1958, 0000 GMT. Notation same as in Fig. 5 a).

The synoptic cases with the worst velocity specifications were often located in the Caribbean Island area. The winds at the lower latitude stations were usually weaker than those at mid-latitudes. Even more important, the winds were not nearly as uniform. Thus, the residual winds and the resultant velocity specification did not seem as accurate here. In Figure 15, a very poor velocity specification comes out of the analysis. The influenced stations still exhibit cyclonic circulation, as do the nearest uninfluenced rawinsonde observations at Jacksonville (088/07), Grand Cayman Island (250/07) and Guantanamo, Cuba (173/08). This particular case seems to be a combination of several error sources. First of all, the low latitude location makes prediction more difficult. Second, not enough storm circulation has been removed. Also, 300 nm was not a particularly good choice for the maximum storm influence distance. And finally, since Miami (055/14) was about 100 nm away from the storm center, the positioning of the storm center was still quite crucial. In fact, with the Miami observation ignored, the specification direction would be improved substantially.

Now, for the cases presented thus far, the large-scale flow has been rather uniform, and the storm track has been steady. This objective procedure also showed excellent specifications for tropical storm Delia, 1973. This especially interesting storm performed a loop along the Texas Gulf Coast and then moved inland. Operational SANBAR forecasts (based on straight uniform large-scale flow representing the most recent

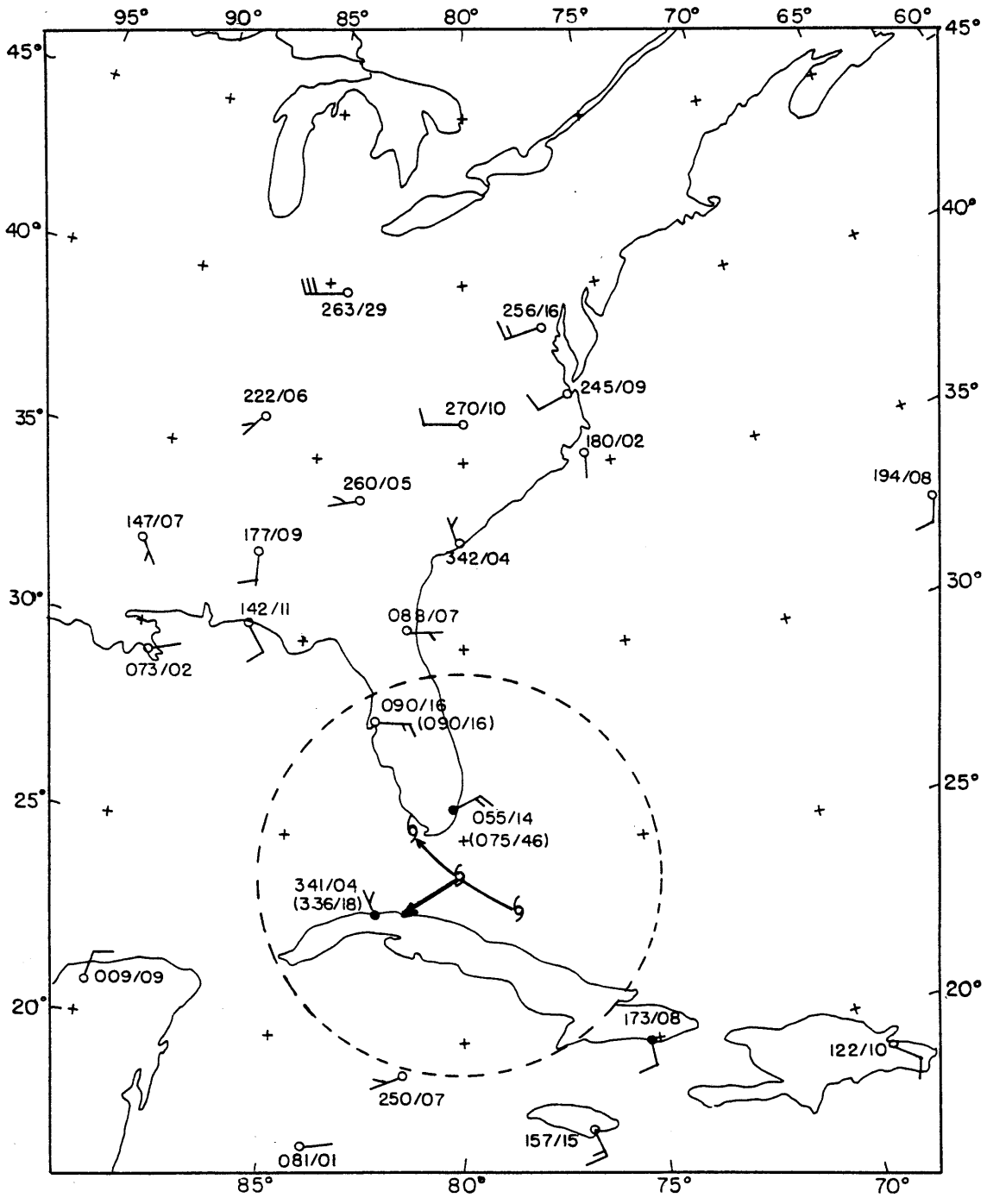

Fig. 15 -- Initial mean layer winds for hurricane Donna, September 10, 1960, 0000 GMT. Notation same as in Fig. 5 a).

storm-track vector) were not able to predict the future storm movement successfully. But this new procedure (which uses the numerous observations within the influence distance) showed excellent specification of the track velocity. In Figure 16 a) the composite storm track and the individual specifications are shown, while in 16 b) the specifications are grouped together to show the counterclockwise change in the specification as the storm looped.

The individual cases which follow (Figures 17 a)-e)) are highlighted by the interaction of Delia with a larger cyclone, denoted by the heavy block letter. The position of the larger cyclone was determined by the lines shown, which separate north residual wind from south, and east from west. As Delia and the larger cyclone circle about each other, the looping motion of Delia seems accountable as a barotropic process.

Figure 16 a)

Velocity specifications for hurricane Delia, September 4-6, 1973

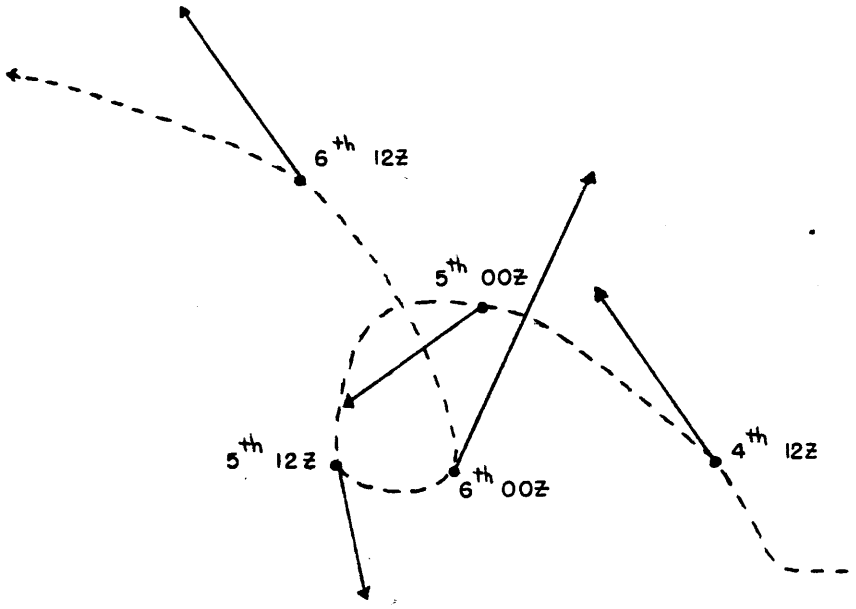

Figure 16 b)

Compilation of velocity specifications for hurricane Delia

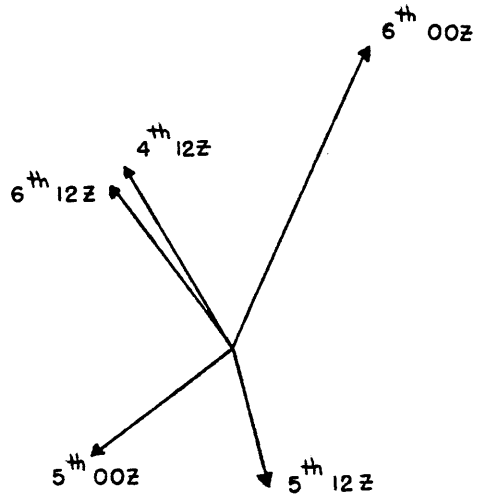

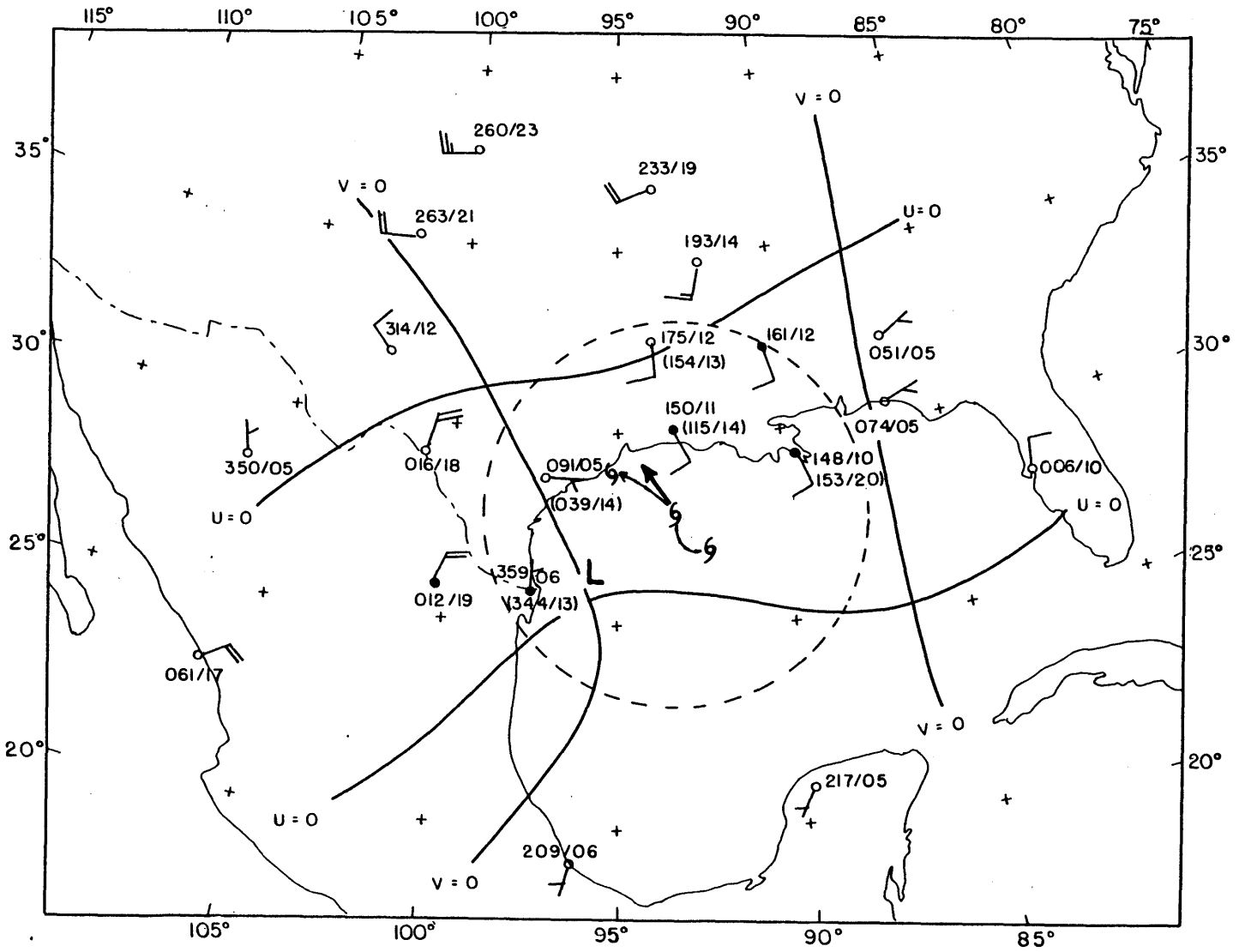

Figure 17 a)

Fig. 17 -- Initial mean layer winds for hurricane Delia, September 1973: a) 4th 1200 GMT, b) 5th 0000 GMT, c) 5th 1200 GMT, d) 6th 0000 GMT, e) 6th 1200 GMT. Notation same as in Fig. 5 a).

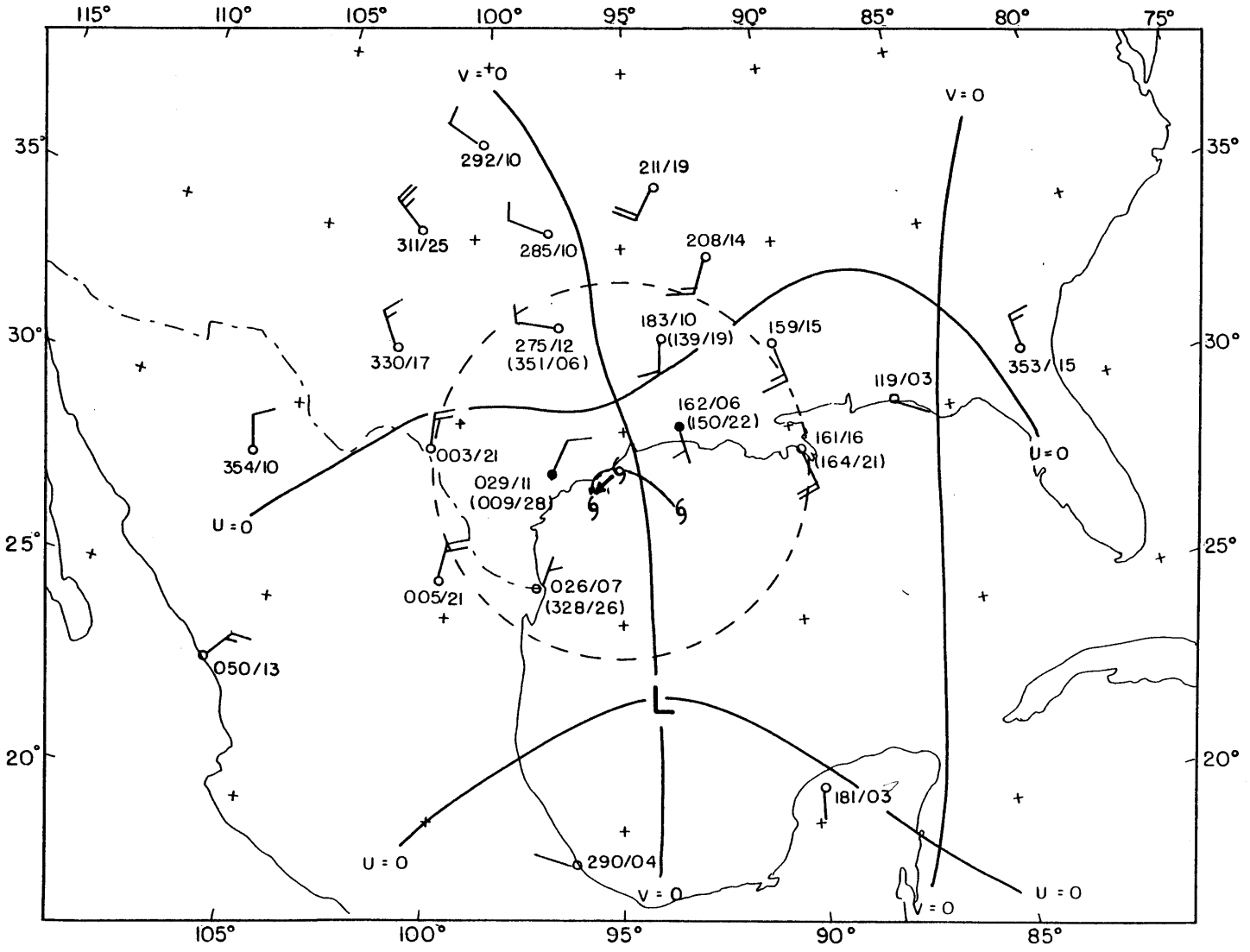
115°
110°
105°
100°
95°
90°
85°
80°
75°
35°
30°
25°
20°
V = 0
292/10
211/19
311/25
285/10
208/14
183/10
(139/19)
159/15
330/17
275/12
(351/06)
353/15
119/03
162/06
(150/22)
354/10
003/21
161/16
(164/21)
029/11
(009/28)
U = 0
005/21
026/07
(328/26)
050/13
181/03
290/04

Figure 17 b)

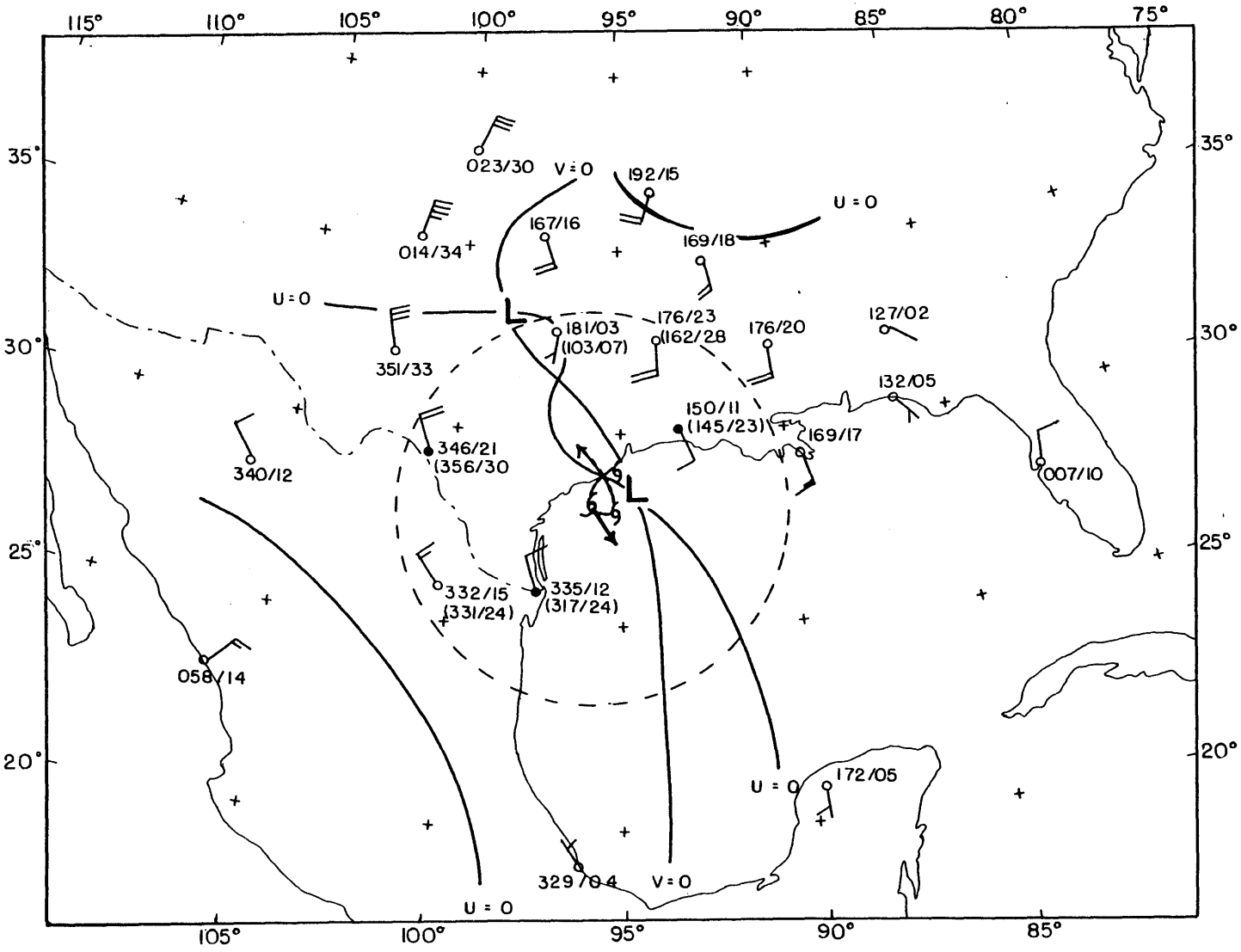
115°
110°
105°
100°
95°
90°
85°
80°
75°
35°
30°
25°
20°
023/30
V=0
192/15
U=0
167/16
014/34
169/18
U=0
176/23
(162/28
181/03
(103/07)
176/20
127/02
351/33
132/05
150/11
(145/23)
169/17
346/21
(356/30
340/12
007/10
332/15
(331/24)
335/12
(317/24)
058/14
U=0
172/05
329/04
V=0
U=0

Figure 17 c)

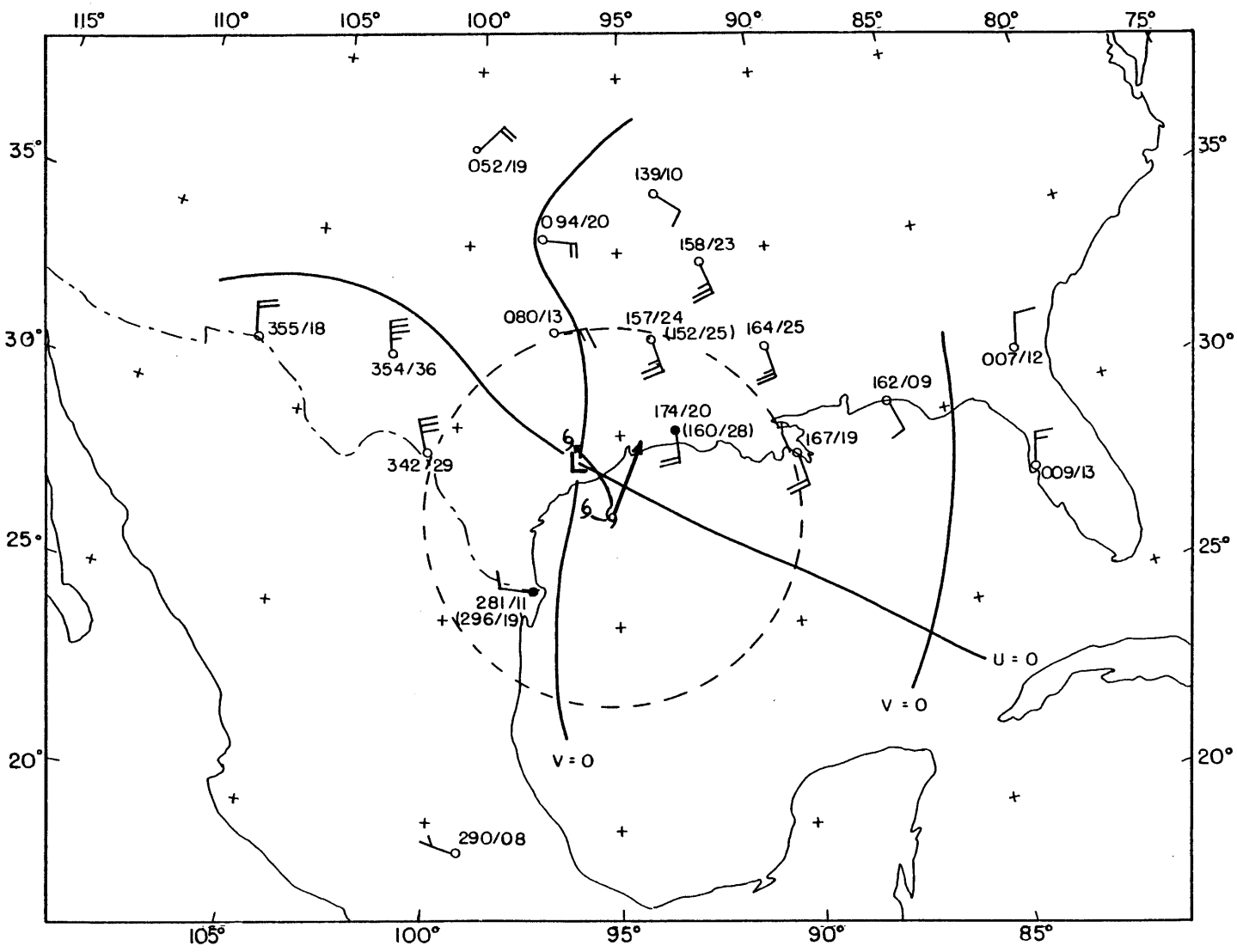
115°
110°
105°
100°
95°
90°
85°
80°
75°
35°
30°
25°
20°
052/19
139/10
094/20
158/23
080/13
157/24
(152/25)
164/25
355/18
354/36
007/12
162/09
174/20
(160/28)
167/19
342/29
009/13
281/11
(296/19)
U = 0
V = 0
V = 0
290/08

Figure 17 d)

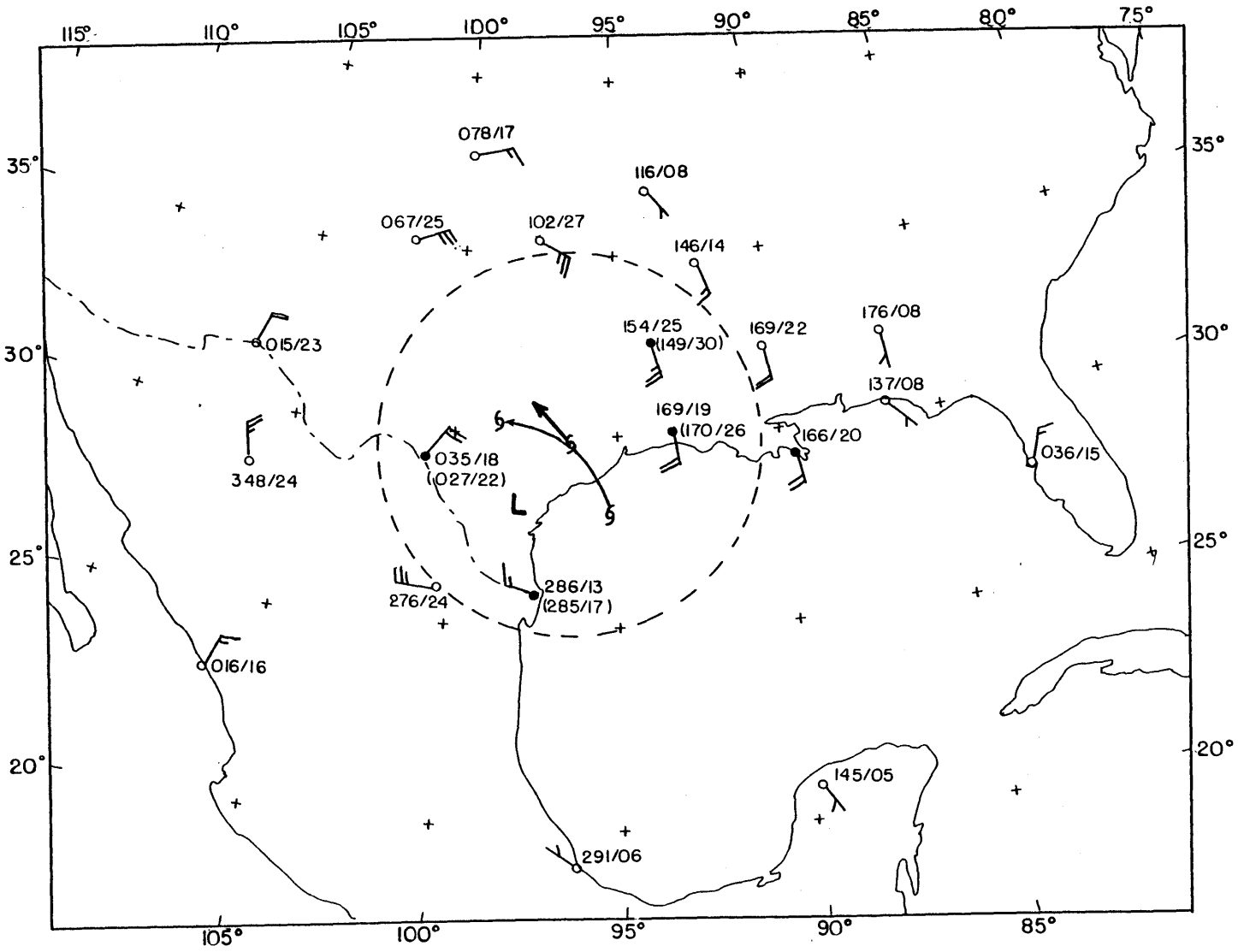
115°
110°
105°
100°
95°
90°
85°
80°
75°
35°
30°
25°
20°
078/17
116/08
067/25
102/27
146/14
176/08
154/25
(149/30)
169/22
015/23
137/08
169/19
(170/26
166/20
348/24
035/18
(027/22)
036/15
286/13
(285/17)
276/24
016/16
145/05
291/06

Figure 17 e)

DISCUSSION AND CONCLUSIONS

The ultimate concern of this study was to improve operational predictions of tropical storm tracks. The focal point was the barotropic filtered model SANBAR, currently in use at NHC. This model performs competitively with the other objective models, despite its neglect of any rawinsonde observations made within 300 nm of the storm center. We felt that a possible way of improving performance was to somehow make effective use of these storm-influenced wind observations.

The first thing needed was a method for separating the vector storm contribution from the layer-mean observed winds. We subtracted 8,000 different storm wind profiles from the observed wind pattern, and the residual pattern which seemed "smoothest" was then used in the remaining analysis. In this manner, we could minimize the occurrence of unreasonable looking residual large-scale winds. Moreover, the observations themselves were used to determine which residual pattern was "smoothest".

Next, the values of the residual wind were used to provide a specification of the storm track velocity at the time of the observations. The specification was determined by stepwise screening regression, given the residual winds at each observing station. Then a comparison was made between this specified track velocity and an estimate of the actual initial velocity. For our fifty case sample, the mean magnitude of the initial velocity was 10 knots, while the

mean magnitude of the vector difference was 4.2 knots. Finally, the regression-specified track velocity was used as a 12-hour extrapolation forecast, and the average position error was 55 nm.

Various factors were then considered to see how they affected the accuracy of the specification. The number of observations within the influence region of the storm seemed to be of minimal importance, while the distance to the nearest observing station was extremely important. In the end, observations within 85 nm of the storm center had to be neglected, because they were overly sensitive to the positioning of the storm center, which can only be roughly estimated for real-time forecasts. On the basis of our results, observations seem most informative when located about 100 nm from the storm center. Better specifications should also result when there is uniform station coverage around the storm center, due to a cancellation of errors.

We recommend that this new procedure be incorporated in the SANBAR analysis for use whenever sufficient rawinsonde data is available in the vicinity of the storm. All our cases involved at least two such rawinsonde observations. This procedure, in which the variability of storm structure is recognized and the observations determine some parameters of the storm circulation itself, appears capable of specifying the initial storm-track velocity about as well as present subjective practise. Its primary potential advantage is that the large-scale flow in the storm-influenced region is not

constrained to be uniform. It should prove to be especially useful when erratic tracks occur close to landfall.

BIBLIOGRAPHY

Ahn, C.S., 1967: Numerical prediction of hurricane movement. MS Thesis, Massachusetts Institute of Technology.

Dunn, G.E., 1961: The hurricane season of 1960. Monthly Weather Review, 89, 99-108.

Dunn, G.E. and Staff, 1959: The hurricane season of 1959. Monthly Weather Review, 87, 441-450.

Dunn, G.E. and Staff, 1964: The hurricane season of 1963. Monthly Weather Review, 92, 128-138.

Gaertner, J.P., 1973: Investigation of forecast errors of the SANBAR hurricane track model. MS Thesis, Massachusetts Institute of Technology.

Herbert, P.J., 1976: Atlantic hurricane season of 1975. Monthly Weather Review, 104, 453-465.

Herbert, P.J. and N.L. Frank, 1974: Atlantic hurricane season of 1973. Monthly Weather Review, 102, 280-289.

Hope, J.R., 1975: Atlantic hurricane season of 1974. Monthly Weather Review, 103, 285-293.

Jordan, E.S., 1952: An observational study of the upper-wind circulation around tropical storms. Journal of Meteorology, 9, 340-346.

King, G.W., 1966: On the numerical prediction of hurricane trajectories. MS Thesis, Massachusetts Institute of Technology.

Miami Weather Bureau Office, 1958: The hurricane season of 1958. Monthly Weather Review, 86, 477-485.

Panofsky, H.A. and G.W. Brier, 1958: Some Applications of Statistics to Meteorology. The Pennsylvania State University, University Park, Pennsylvania, 224 pp.

Pike, A.C., 1972: Improved barotropic hurricane track prediction by adjustment of the initial wind field. NOAA Technical Memorandum NWS SR-66.

Riehl, H., W.H. Haggard, and R.W. Sanborn, 1956: On the prediction of 24-hour hurricane motion. Journal of Meteorology, 13, 415-420.

Sanders, F., 1970: Dynamic forecasting of tropical storm tracks. Transactions of the New York Academy of Sciences, 32, 495-508.

Sanders, F. and R.W. Burpee, 1968: Experiments in barotropic hurricane forecasting. Journal of Applied Meteorology, 7, 313-323.

Sanders, F., A.C. Pike, and J.P. Gaertner, 1975: A barotropic model for operational prediction of tracks of tropical storms. Journal of Applied Meteorology, 14, 265-280.

Sanders, F. and N.J. Gordon, 1976: A study of forecast errors in an operational model for predicting paths of tropical storms. Scientific Report No. 2, Contract F19628-75-C-0059 AFGL-TR-77-0079.

Simpson, R.H., A.L. Sugg, and Staff, 1970: The Atlantic hurricane season of 1969. Monthly Weather Review, 98, 293-306.

Williams, F.R., 1972: Applications of the SANBAR hurricane track forecast model. MS Thesis, Massachusetts Institute of Technology.